Anatomically accurate modelling of electrical and mechanical function of the heart

Alexander Panfilov, Gent University, Belgium

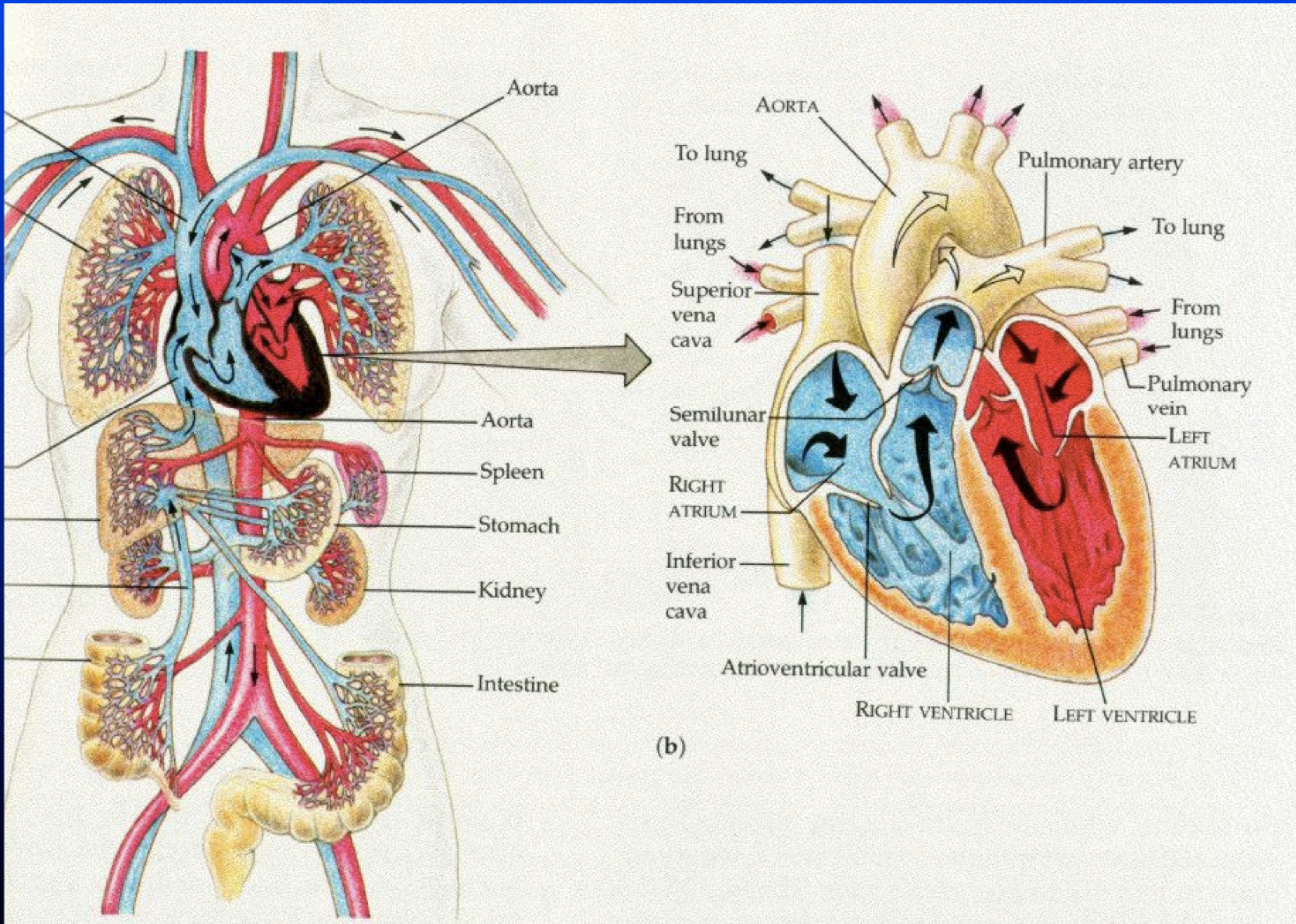

Aorta
Aorta
Spleen
Stomach
Kidney
Intestine
AORTA
To lung
Pulmonary artery
From lungs
To lung
Superior vena cava
From lungs
Pulmonary vein
Semilunar valve
LEFT ATRIUM
RIGHT ATRIUM
Inferior vena cava
Atrioventricular valve
RIGHT VENTRICLE
LEFT VENTRICLE

(b)

Normal excitation of the heart

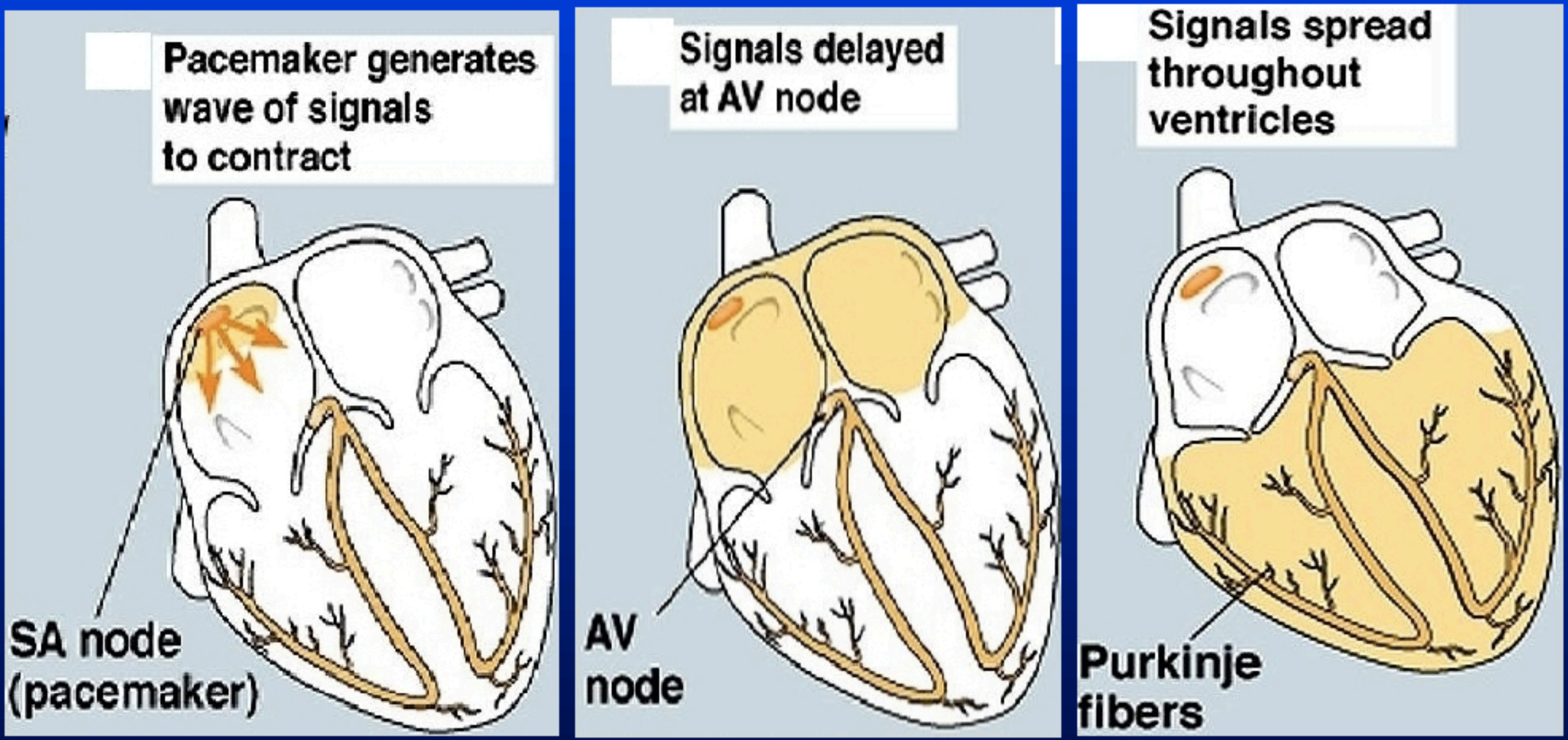

Some types of arrhythmias

- Ectopic beats. The heart has an extra beat. Treatment usually is not needed.
- Paroxysmal atrial tachycardia. The heart has episodes when it beats fast, but regularly. This type of arrhythmia may be unpleasant but is usually not dangerous.
- Atrial fibrillation. The heart beats too fast and irregularly. This type of arrhythmia requires treatment and can increase your risk of stroke.
- Ventricular tachycardia and ventricular fibrillation. The heart beats too fast and may not pump enough blood. These types of arrhythmias are very dangerous and need immediate treatment.

VF epidemiology

VF is the single largest categorical cause of natural death in the Western hemisphere.

If accounts for about 450 000 sudden deaths in the US annually

(Zhi-Jie Zheng et al., Circulation. 2001 Oct 30;104(18):2158-63.)

BASIC PROPERTIES OF CARDIAC EXCITATION

- Conduction
- Refractoriness (time during which a second wave cannot be initiated)

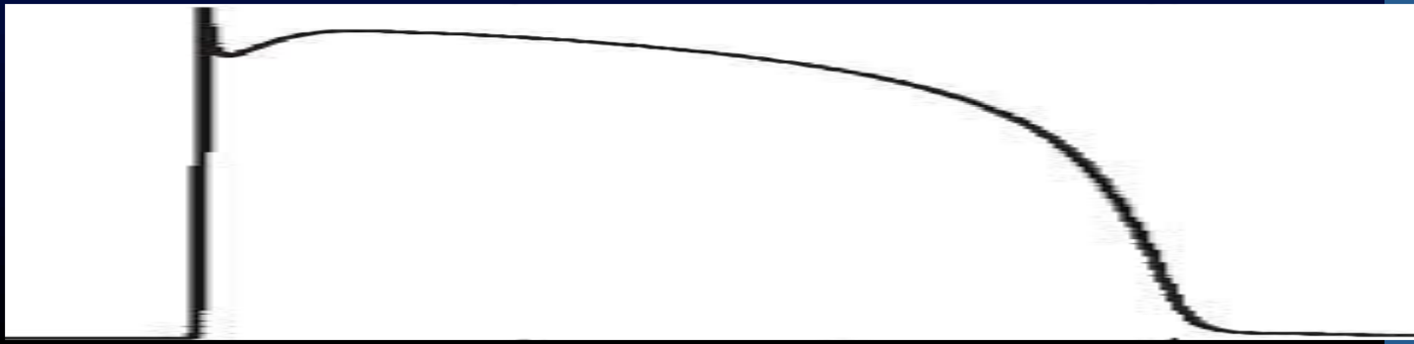

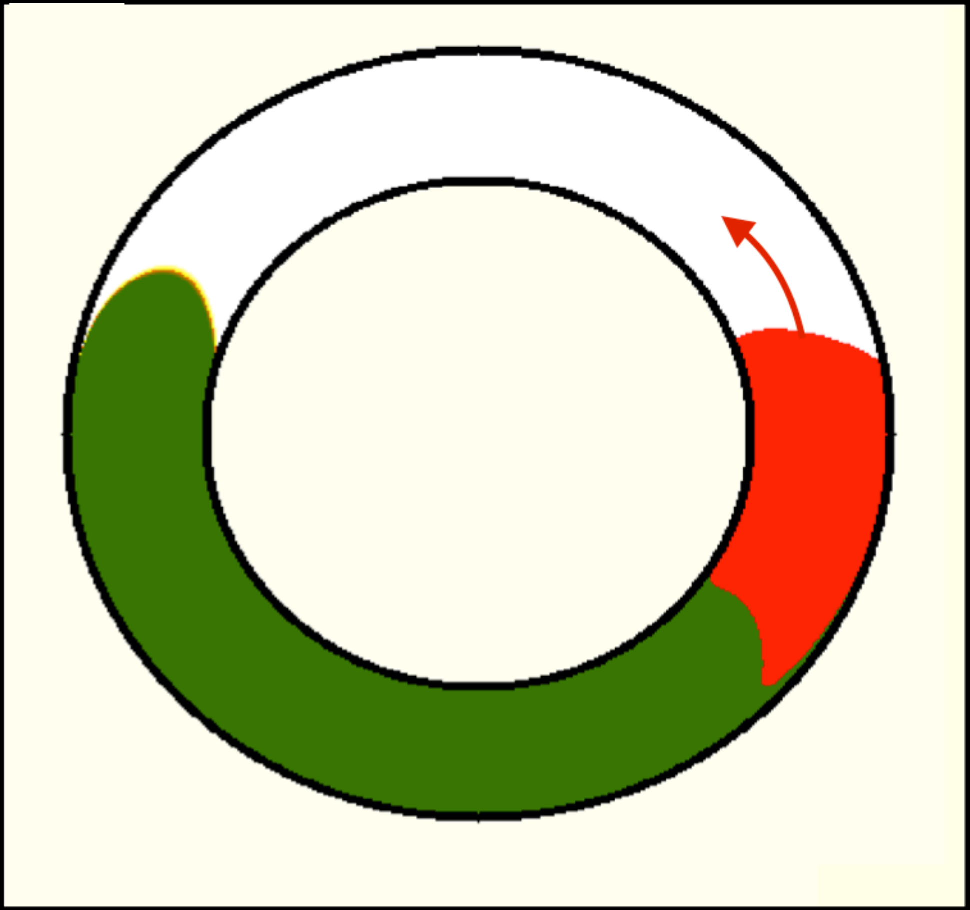

Wave can circulation of pulse in a ring of the length L
if L>R*v (refractory period times velocity)

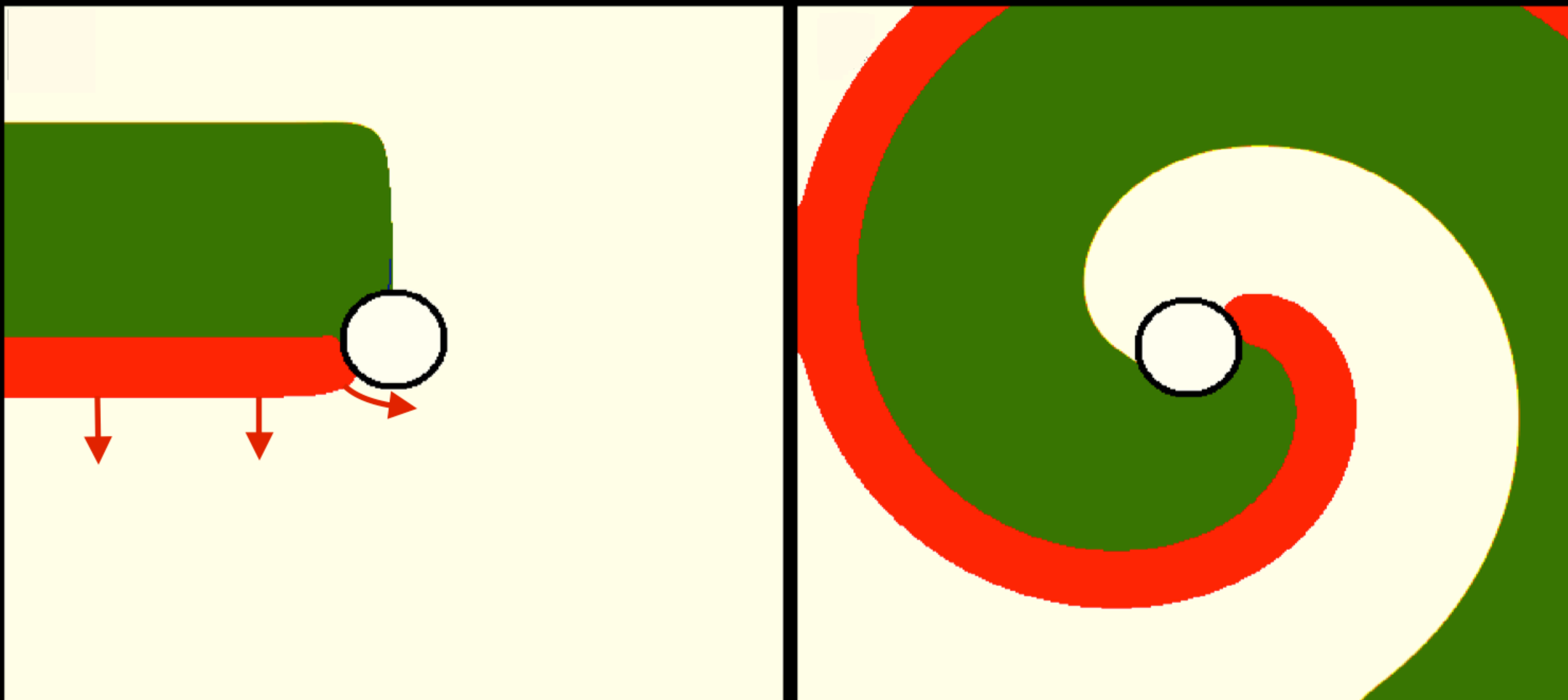

In 2D we obtain a wave of spiral shape rotating around an obstacle
Period is determined by the ovstacle size L and wave velocity v: T=L/v

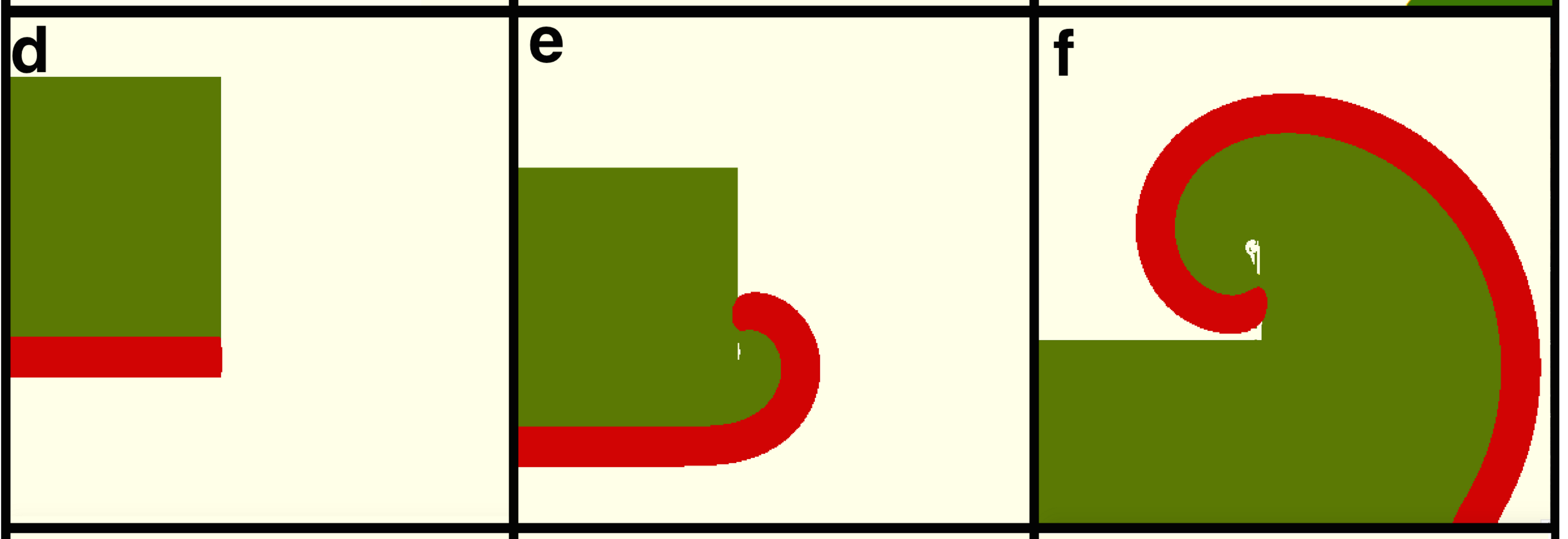

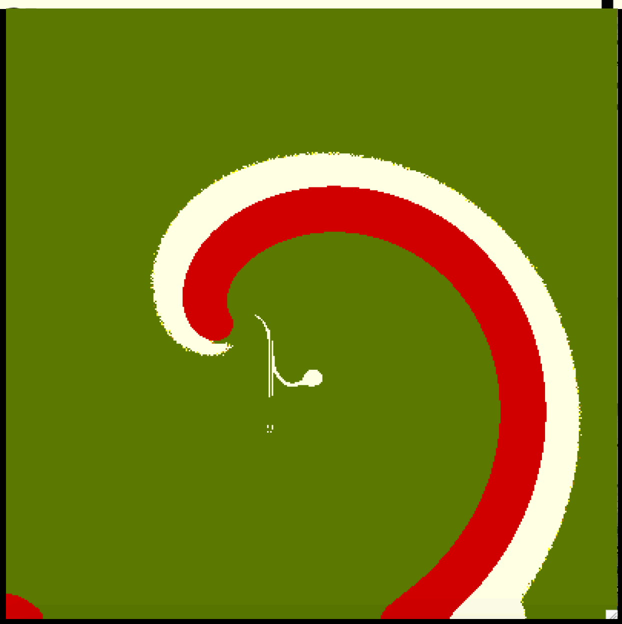

Period is determined by the refractory period R: T≅R

Scroll wave and its filament

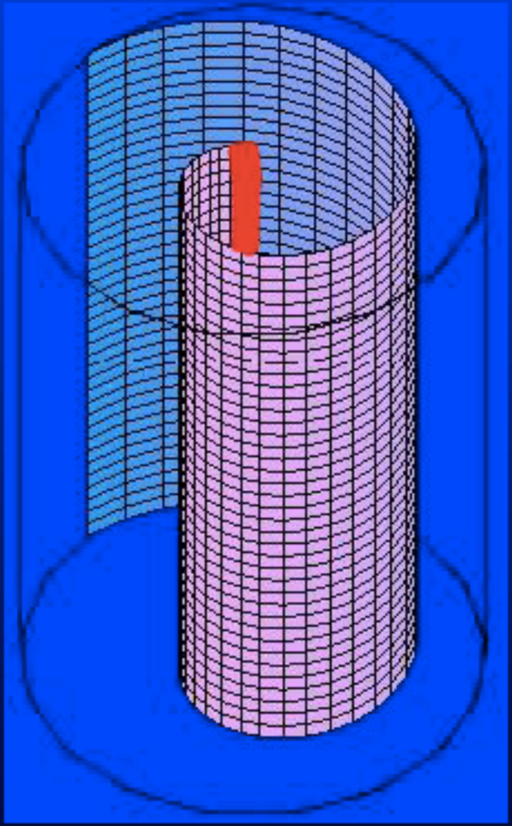

Sources of an arrhythmia and fibrillation

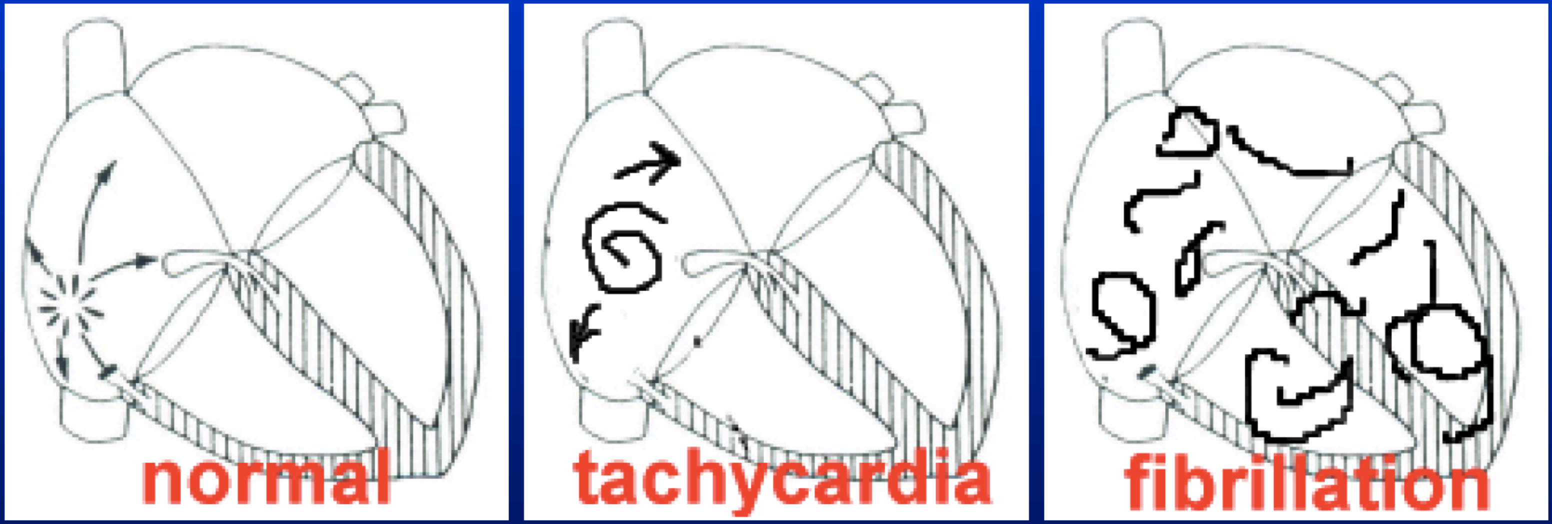

Cardiac arrhythmias → millions of cells

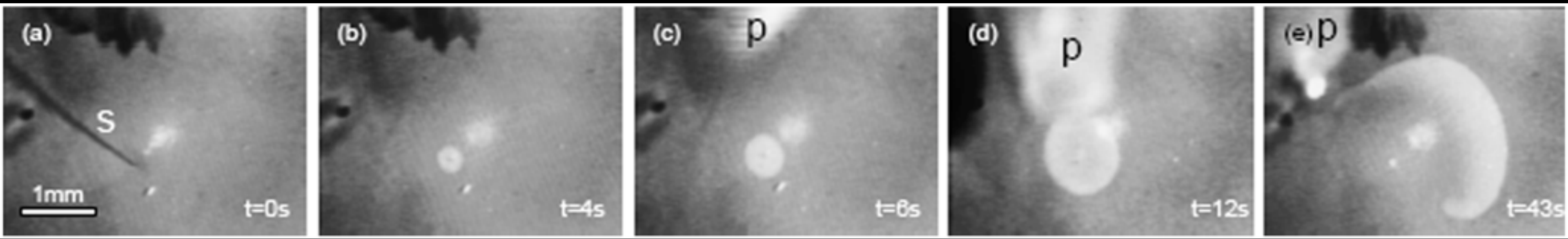

00:00:00

Virtual heart

Cell $\rightarrow$ Tissue $\rightarrow$ Organ

allows us to

- extend one cell $\rightarrow$ whole organ
- study excitation in 3D
- study arrhythmias in human heart

Cell models: $2 \sim 100$ ODEs

$$\begin{cases} C_m \frac{\partial V_m}{\partial t} & = -I_m(V_m, g_i) \\ I_m & = I_{Na} + I_K + I_{Leak} + \ldots \\ \frac{dg_i}{dt} & = \frac{g_{i\infty}(V_m) - g_i}{\tau_{g_i}(V_m)} \end{cases}$$

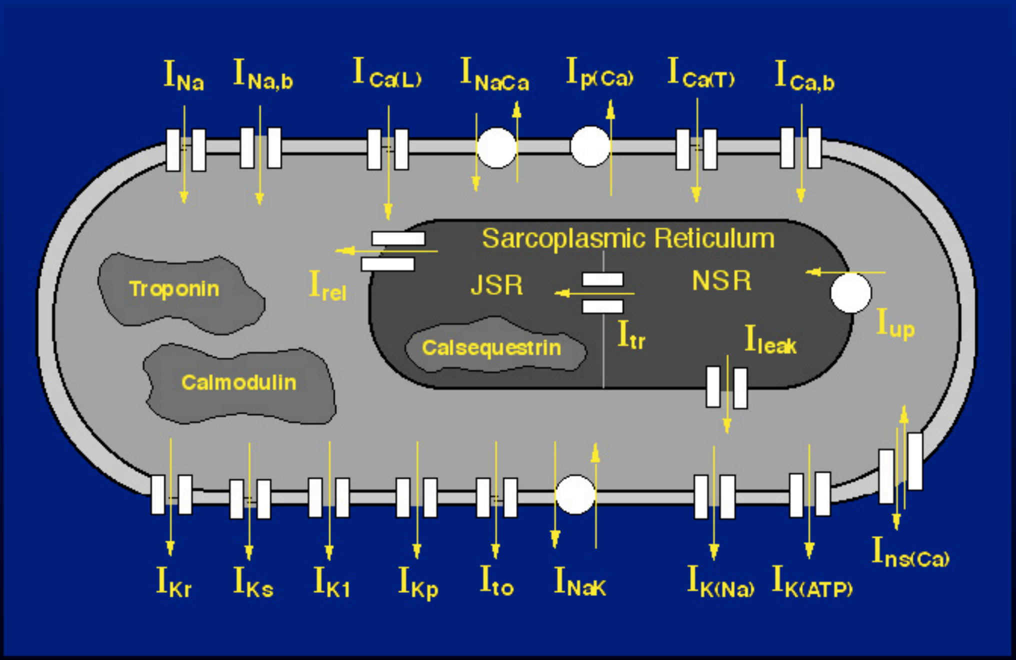

Ionic current description

$$
\begin{cases}
I_m = I_{Na} + I_K + I_{Leak} + \dots \\
I_{Na} = G_{Na} m^3 h j (V - E_{Na}) \\
\frac{dm}{dt} = \frac{m_\infty(V) - m}{\tau(V)} \\
\dots.
\end{cases}
$$

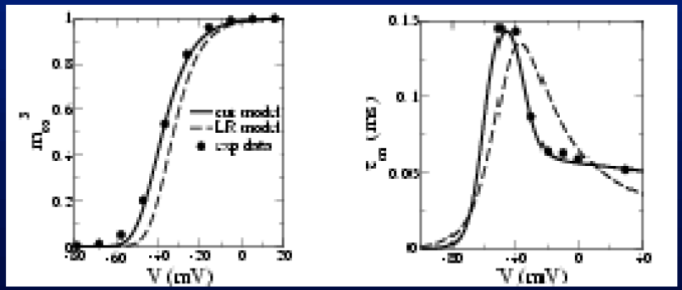

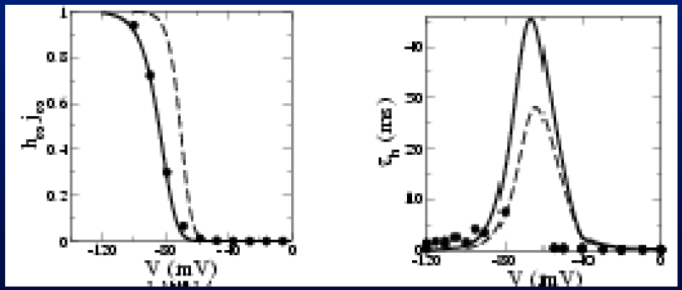

Steady-state and time constants of gating variables for I_{Na} (from: ten Tusscher et al.,AJP,2004,284,H1573-1589)

Cardiac tissue models: monodomain

$$\frac{\partial V_m}{\partial t} = div\mathbf{D}gradV_m - I_m(V_m, g_i)$$

$$\frac{dg_i}{dt} = \frac{g_{i\infty}(V_m)-g_i}{\tau_{g_i}(V_m)}$$

$$d = \begin{pmatrix} d_{11} & d_{12} & d_{13} \\ d_{21} & d_{22} & d_{23} \\ d_{31} & d_{32} & d_{33} \end{pmatrix}$$

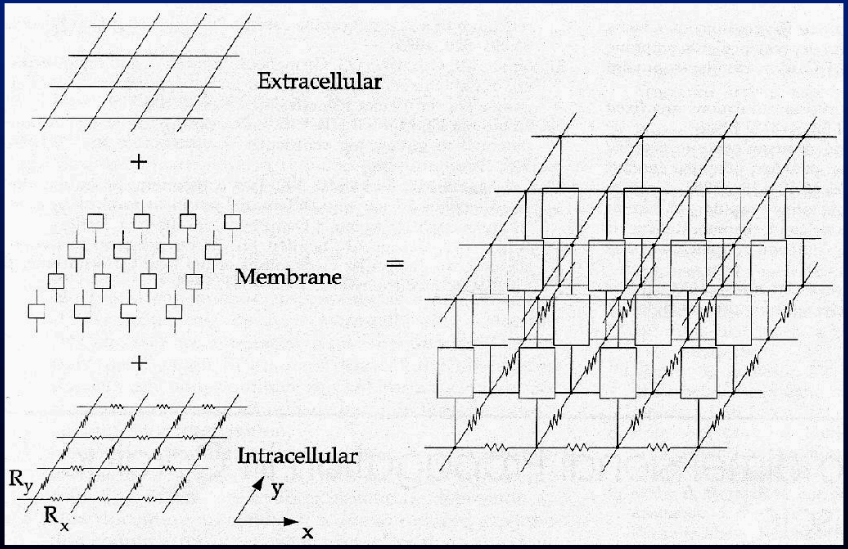

Riemannian space and anisotropy

Laplacian in anisotropic medium

$$\frac{\partial}{\partial X_M}\left(D_{MN}\frac{\partial \mathbf{V}}{\partial X_N}\right) \qquad (1)$$

Laplacian in isotropic medium in curvilinear system with a metric tensor g_{MN}

$$\frac{1}{\sqrt{g}}\frac{\partial}{\partial X_M}\left(\sqrt{g}g^{-1}_{MN}\frac{\partial \mathbf{V}}{\partial X_N}\right) \qquad (2)$$

Where g is $det(g_{MN})$.

If $g_{MN} = D^{-1}_{MN}$ provided $det(D_{MN}) = const$ (1)=(2)

Law of motion for wave fronts in anisotropic media

Extended velocity-curvature relation

$$c = c_0 - \gamma \mathrm{Tr}\mathbf{K} - \eta \partial_\rho \mathrm{Tr}\mathbf{K} - \zeta(\mathrm{Tr}\mathbf{K})^2 + \mathcal{O}(\lambda^3). \tag{9}$$

HD, O. Bernus & H. Verschelde, Phys Rev Lett, 2011.

- Discussion:
  1. Distances rescaled with metric tensor $g_{ij} = D_0(\mathbf{D}^{-1})_{ij}$
  2. Covariant curvature measure: extrinsic curvature tensor $\mathbf{K}$:

$$\mathcal{D}_A \vec{e}_\rho = K_A{}^B \vec{e}_B, \qquad \mathrm{Tr}\,\mathbf{K} = \mathrm{K}_\mathrm{A}{}^\mathrm{A} \tag{10}$$

  3. Explicit coefficients γ, ζ, η known from 1D propagation

$$\gamma = \langle \mathbf{Y} | \hat{P} | \psi \rangle, \qquad \eta = \langle \mathbf{Y} | \rho \hat{P} | \psi \rangle + 2 \langle \mathbf{Y} | \hat{P} | \mathbf{u}_1 \rangle, \tag{11}$$

$$\mathbf{u}_1 = \hat{L}^{-1}\left(\hat{P} - \gamma\right) | \psi \rangle, \quad \zeta = \langle \mathbf{Y} | \left(\hat{P} - \gamma\right) \partial_\rho | \mathbf{u}_1 \rangle - \frac{1}{2} \langle \mathbf{Y} \mid \mathbf{u}_1 \mathbf{F}''(\mathbf{u}_0) \mathbf{u}_1 \rangle$$

  4. Intrinsic curvature of space (Riemann tensor) does not enter law of motion directly

Results on filaments: law of motion (anisotropic)

Lowest order filament dynamics *Verschelde et al., PRL, 2007*

$$\dot{\vec{X}} = \gamma_1\, \mathcal{D}_\sigma^2 \vec{X} + \gamma_2\, \mathcal{D}_\sigma \vec{X} \times \mathcal{D}_\sigma^2 \vec{X} + \mathcal{O}(\lambda^3)$$

- Discussion:
  1. Stationary solutions need $\mathcal{D}_\sigma^2 \vec{X} = 0 \Rightarrow$ geodesics!
     $\Rightarrow$ proves *Minimal principle for rotor filaments*
  2. Higher order corrections (tidal forces) may violate Minimal Principle

PHYSICAL REVIEW E 88, 012908 (2013)

Drift laws for spiral waves on curved anisotropic surfaces

Hans Dierckx,[*] Evelien Brisard, Henri Verschelde, and Alexander V. Panfilov

$$\partial_t \phi = \omega_0 + q_0 \mathcal{R} + O(\lambda^4),$$

$$\partial_t \vec{X} = -q_1 \operatorname{grad} \mathcal{R} - q_2 \vec{n} \times \operatorname{grad} \mathcal{R},$$

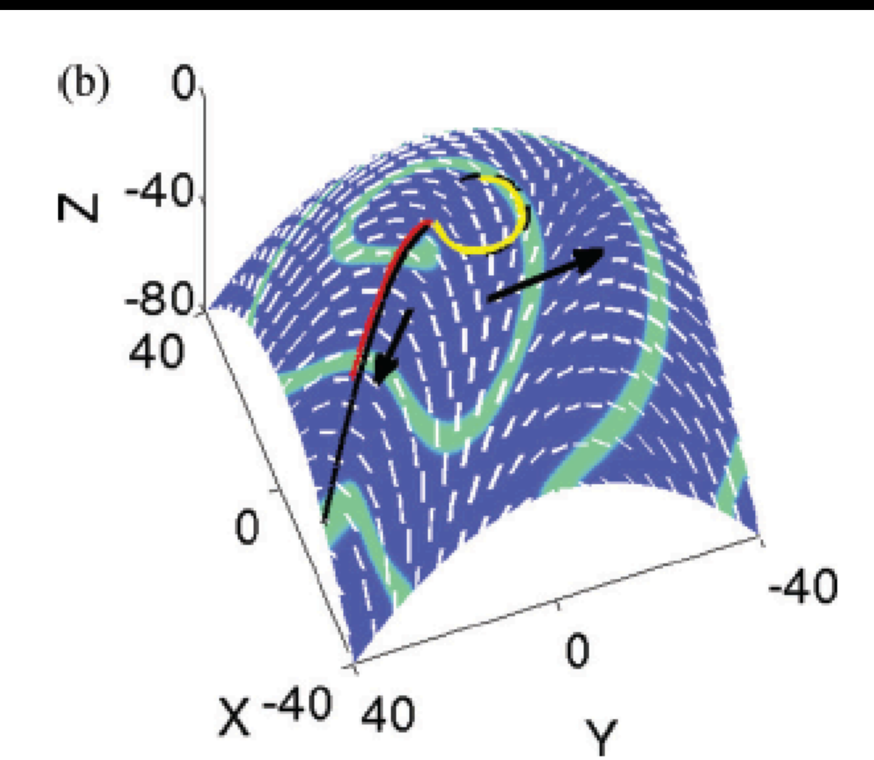

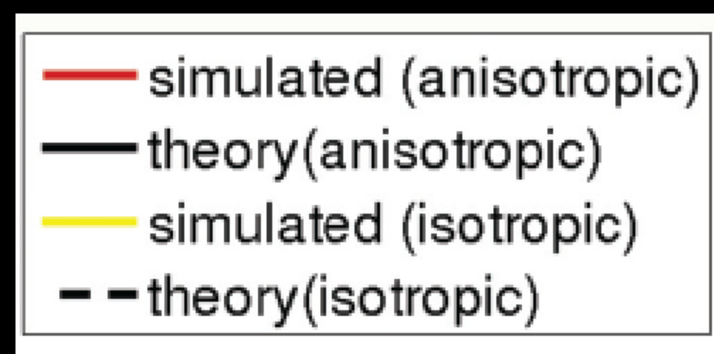

Whole organ models

The diffusion tensor is given by the fiber orientation field α_i as:

$$d_{ij} = d_2 * \delta_{i,j} + (d_1 - d_2)\alpha_i\alpha_j.$$

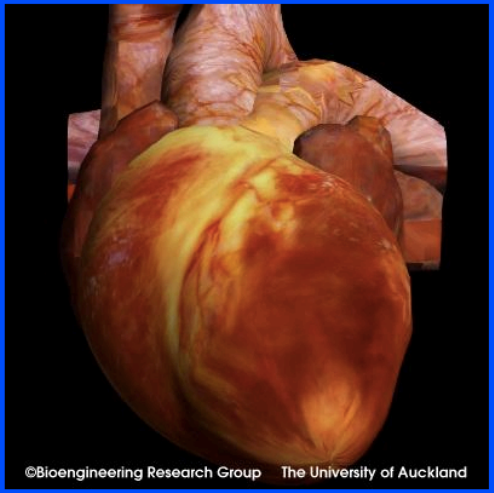

+

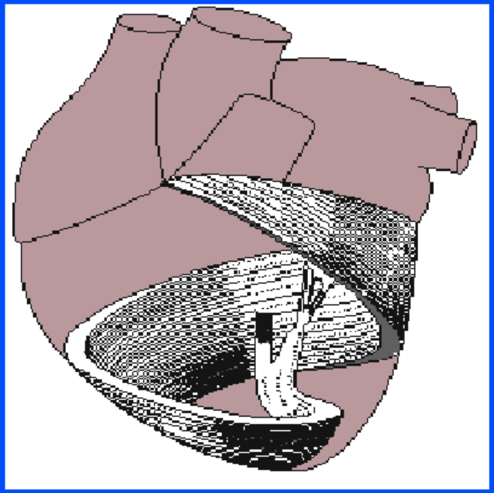

Anatomical data (Nielsen,LeGrice, Smaill and Hunter,1991)

Model of human ventricles

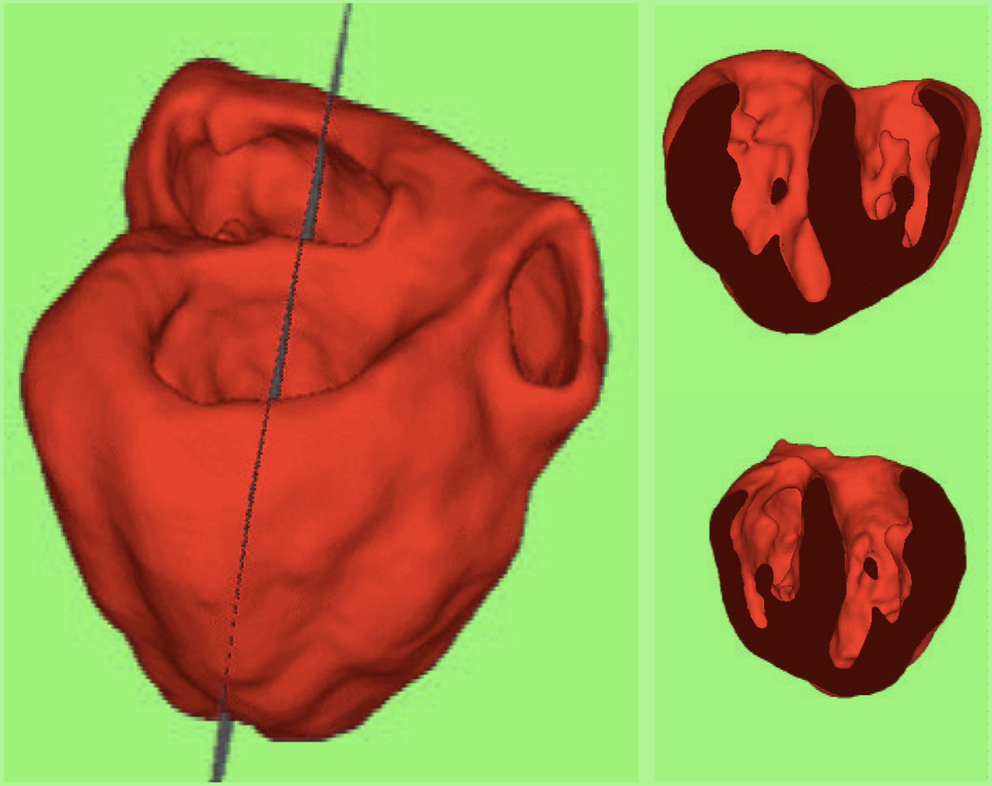

Anatomical data on ventricles of human heart (R.Hren,1996)

A model of the human ventricular myocyte

- Bernus, Wilders, Zemlin, Verschelde, Panfilov, AJP, v.282:H2296-308, 2002
- Bernus, Verschelde, Panfilov, Phys Med Biol., v.47:1947-59, 2002
- Ten Tusscher, Noble, Noble, Panfilov AJP 286: H1573-H1589, 2004
- Ten Tusscher, Panfilov AJP, v.291, p.H1088-1100, 2006

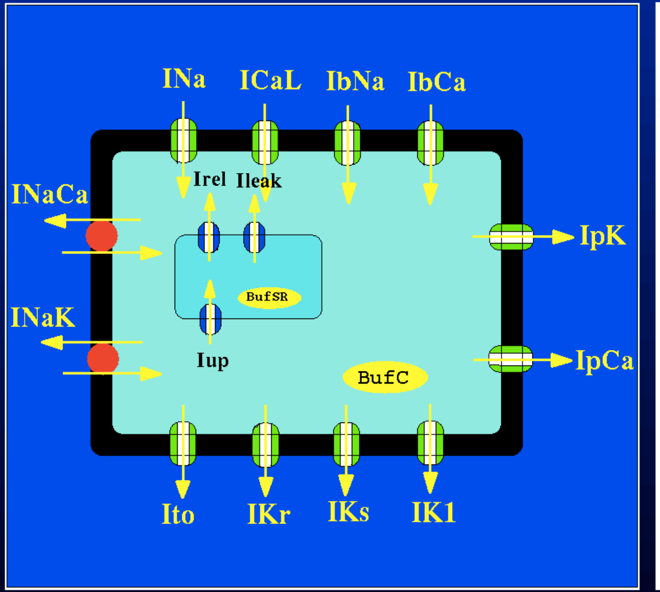

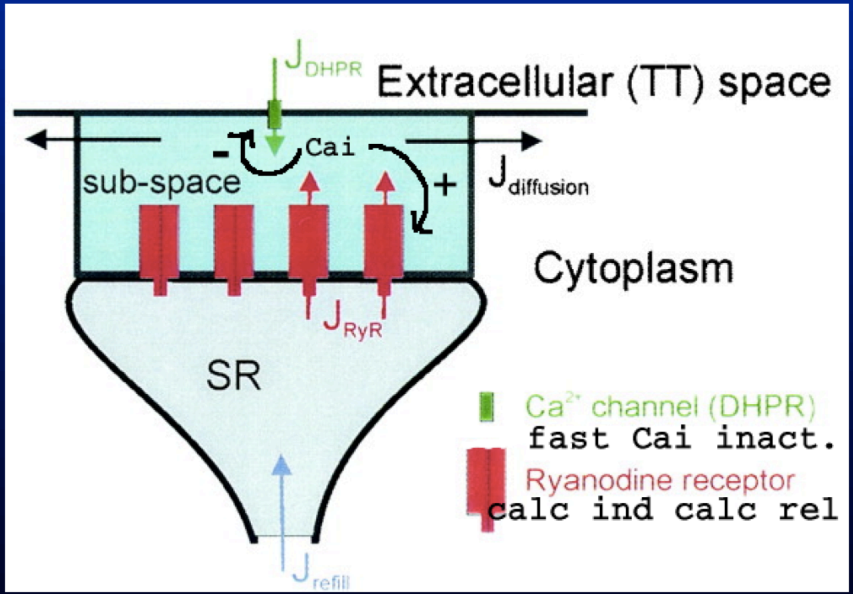

Clinical data on VF sources

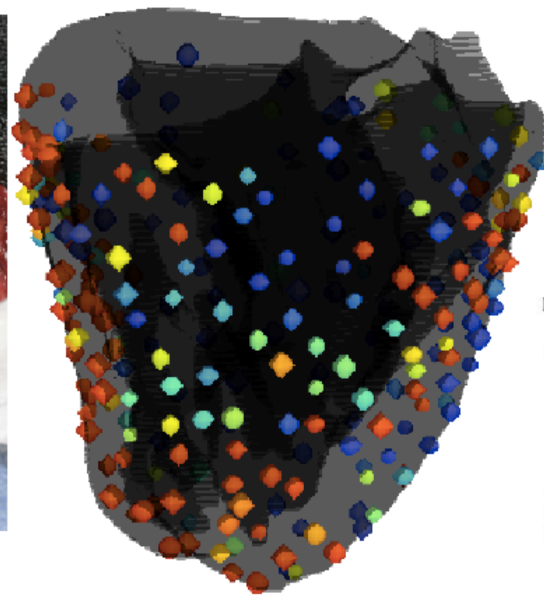

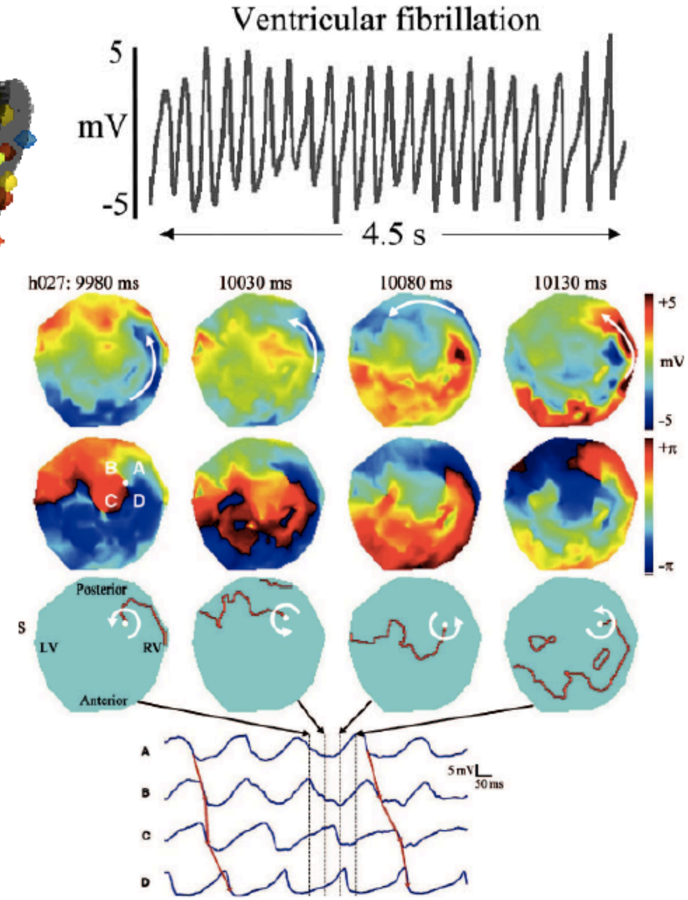

from Nash et al.
Circulation,v.114:536-542,2006

OPEN ACCESS Freely available online

PLOS | COMPUTATIONAL BIOLOGY

Effect of Global Cardiac Ischemia on Human Ventricular Fibrillation: Insights from a Multi-scale Mechanistic Model of the Human Heart

Ivan V. Kazbanov[1], Richard H. Clayton[2,3], Martyn P. Nash[4,5], Chris P. Bradley[4], David J. Paterson[6], Martin P. Hayward[7], Peter Taggart[7], Alexander V. Panfilov[1,8]*

1 Department of Physics and Astronomy, Ghent University, Ghent, Belgium, **2** INSIGNEO Institute for In-Silico Medicine, University of Sheffield, Sheffield, United Kingdom, **3** Department of Computer Science, University of Sheffield, Sheffield, United Kingdom, **4** Auckland Bioengineering Institute, University of Auckland, Auckland, New Zealand, **5** Department of Engineering Science, University of Auckland, Auckland, New Zealand, **6** Department of Physiology, Anatomy and Genetics, University of Oxford, Oxford, United Kingdom, **7** Departments of Cardiology and Cardiothoracic Surgery, University College Hospital, London, United Kingdom, **8** Moscow Institute of Physics

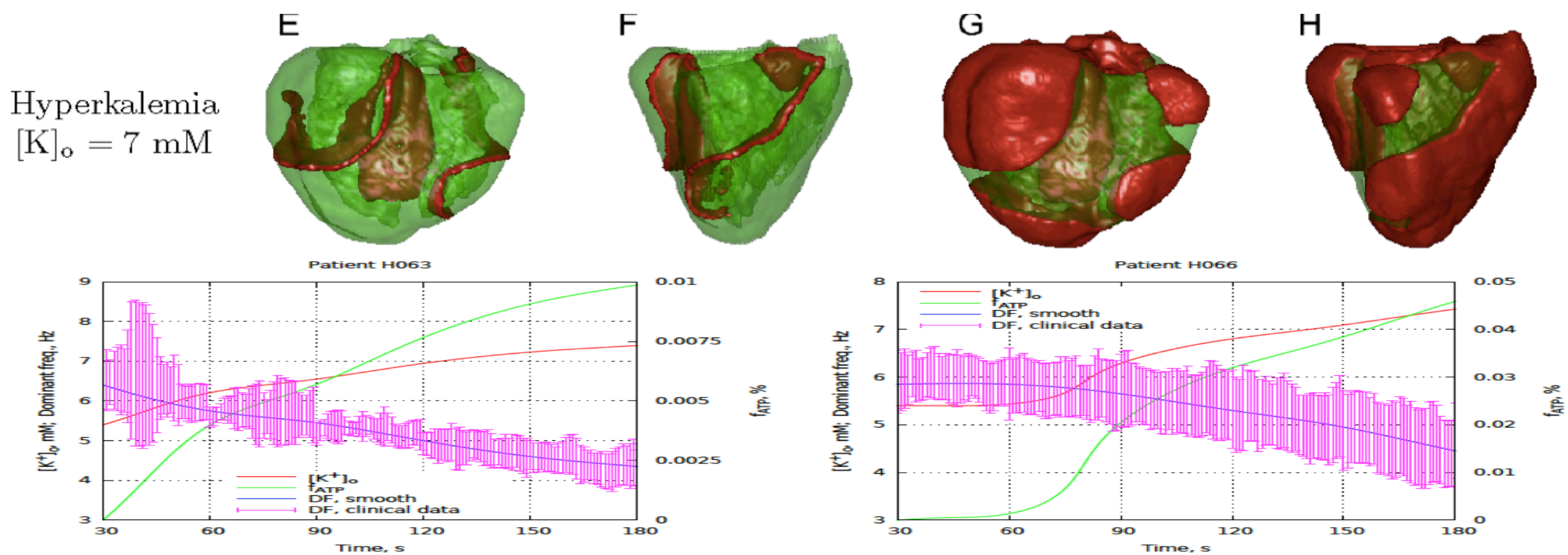

excitation $\longrightarrow$ contraction

Cardiac Resynchronization Therapy (CRT)

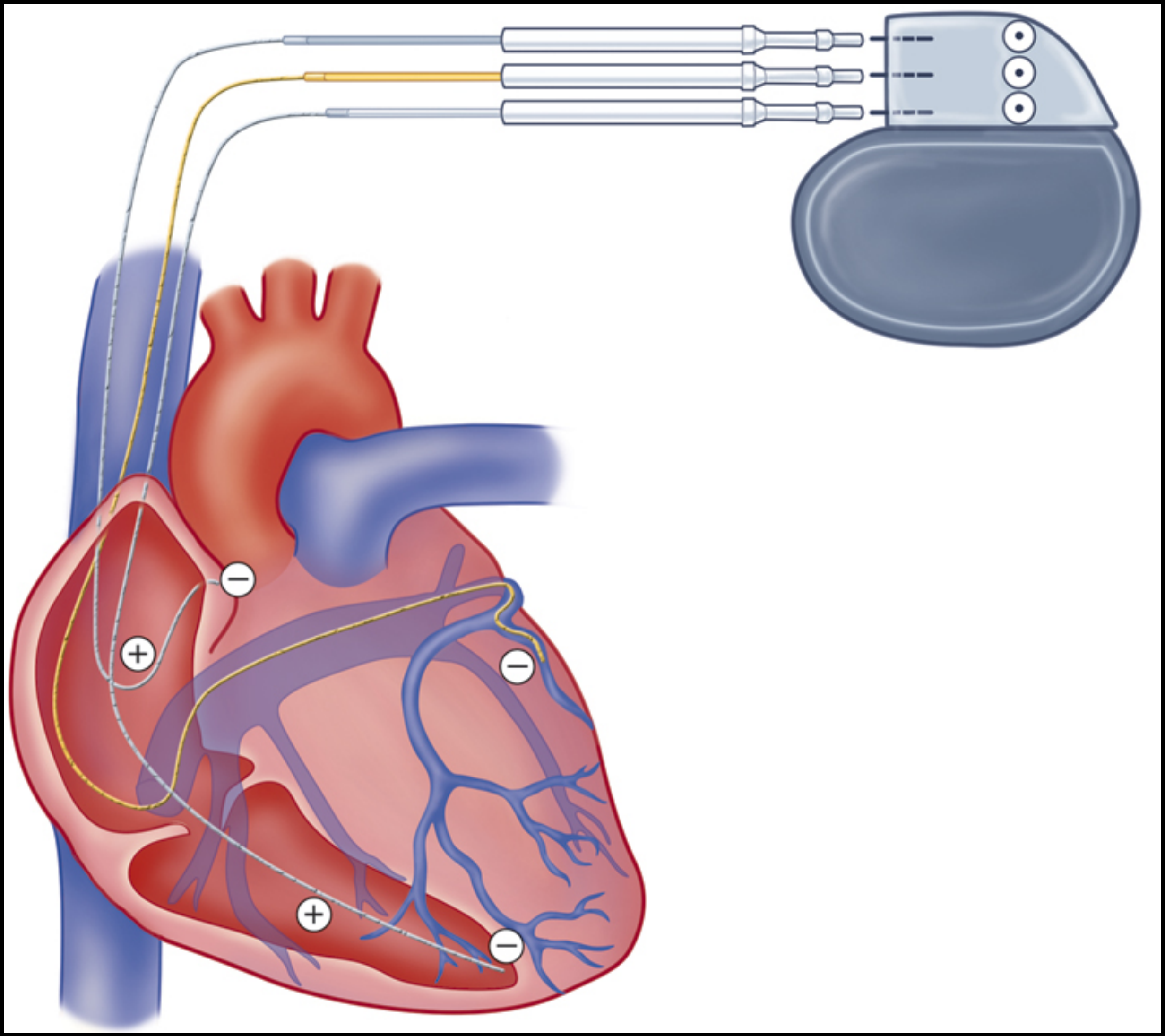

$$\begin{tikzcd}
\text{excitation} \arrow[rr] & & \text{contraction} \arrow[dl, bend left] \\
& \textbf{MEF} \arrow[ul, bend left] &
\end{tikzcd}$$

excitation → contraction

MEF

arrhythmogenic (commotio cordis)

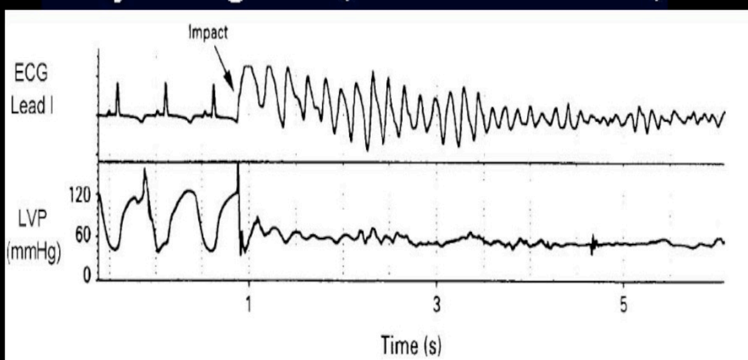

life saving (precordial thump)

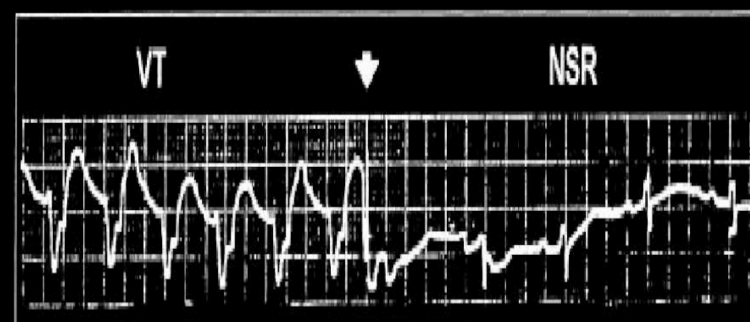

Mechanical stimulation

(From Franz et al, Circulation, 1992)

Coupled Reaction-diffusion-mechanics systems

- RD system:

$$\partial \mathbf{V}/\partial t = div(\mathbf{D} grad \mathbf{V}) + \mathbf{F}(\mathbf{V}, \mathbf{E})$$

- mechanics:

$$\frac{\partial}{\partial X_M}(T^{MN}\frac{\partial x_j}{\partial X_N}) = 0$$

- constitutive relations:

$$T^{MN} = T_p^{NM}(\mathbf{E}) + T_a^{NM}(\mathbf{E}, \mathbf{V})$$

T^{MN}- is a second Piola-Kirchhoff stress tensor,
$\mathbf{E}$- is the Green's strain tensor,
T_p^{NM}, T_a^{NM}- are passive and active stress tensors.

Nash and Panfilov PBMB 2004

Deformation induces breakup and drift of spiral waves

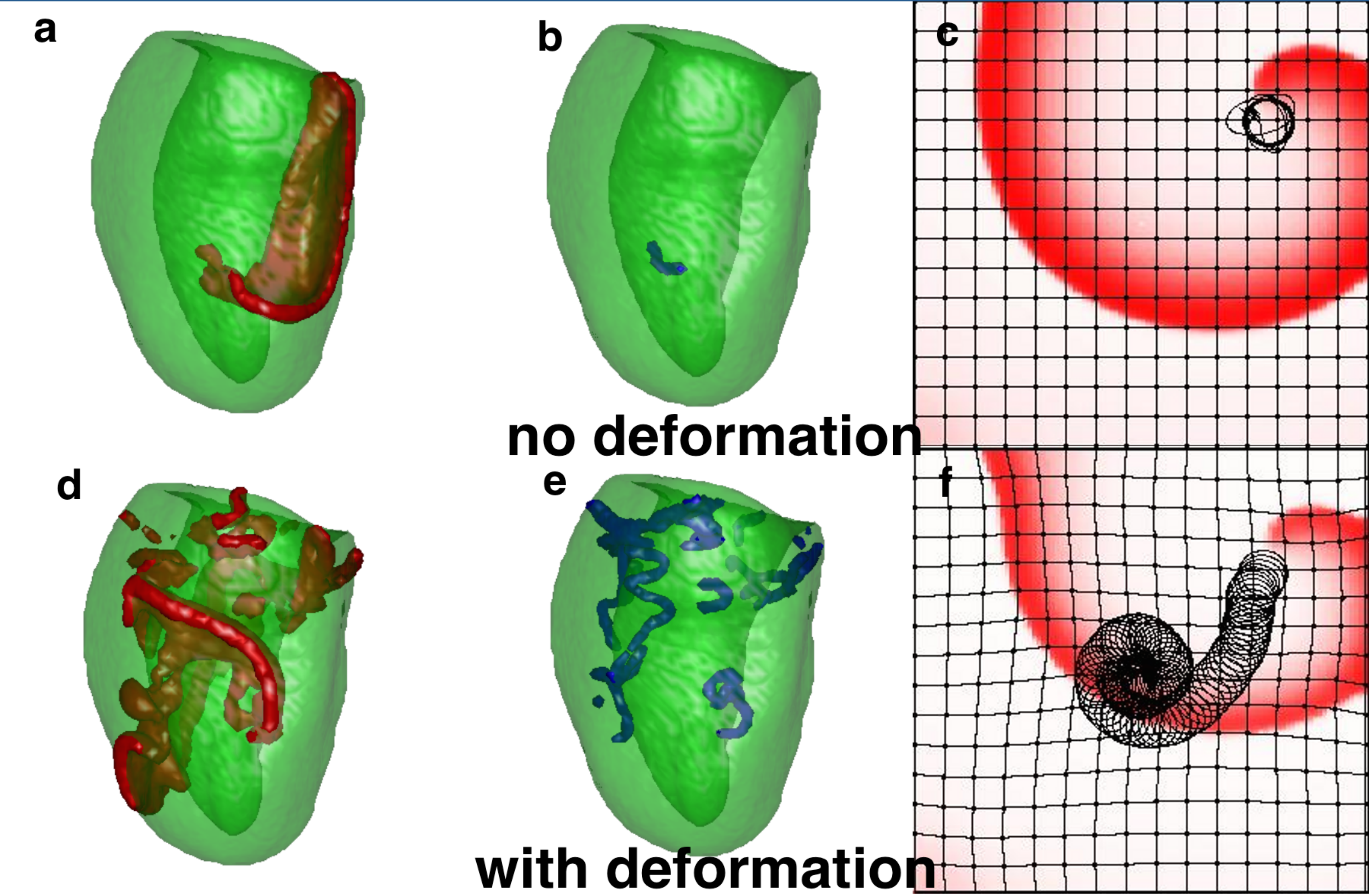

Multiphysics cardiac modelling

Multiphysics cardiac modelling

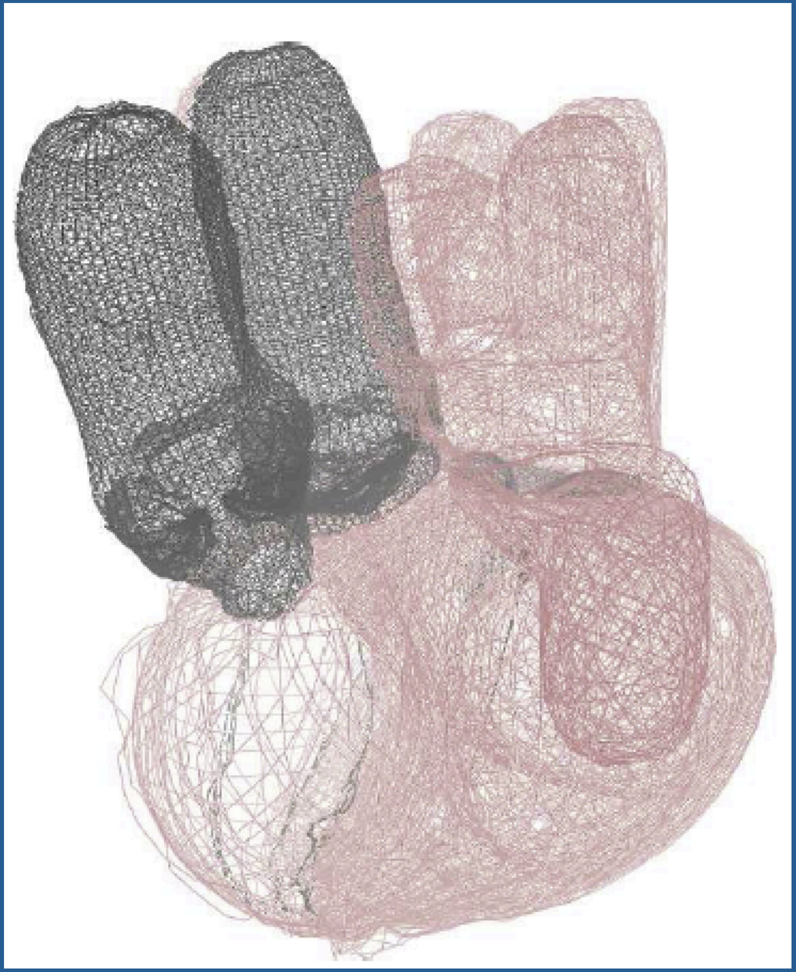

Griffith and Peskin

Multiphysics cardiac modelling

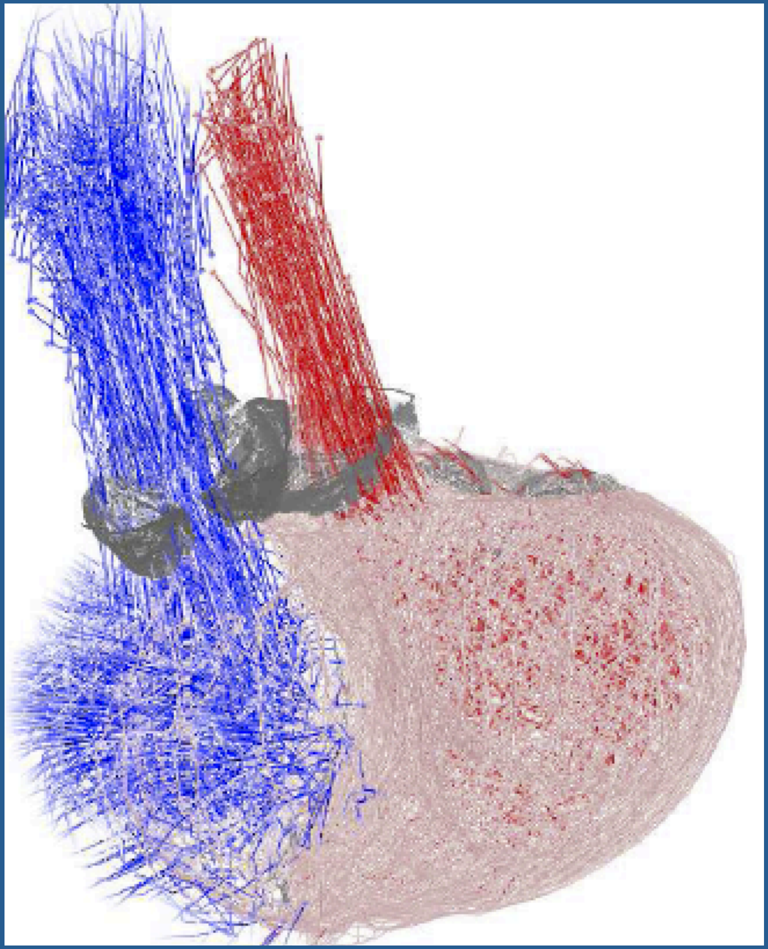

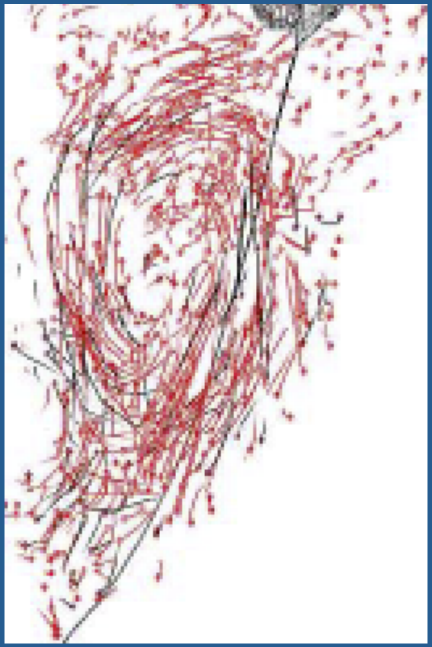

Flow in LV

RV

Griffith and Peskin

Dynamical anchoring of cardiac arrhythmias

Alexander Panfilov, Ivan Kazbanov, Nele Vandersickel, Arme Defauw

The human heart Physiology Program Washington University

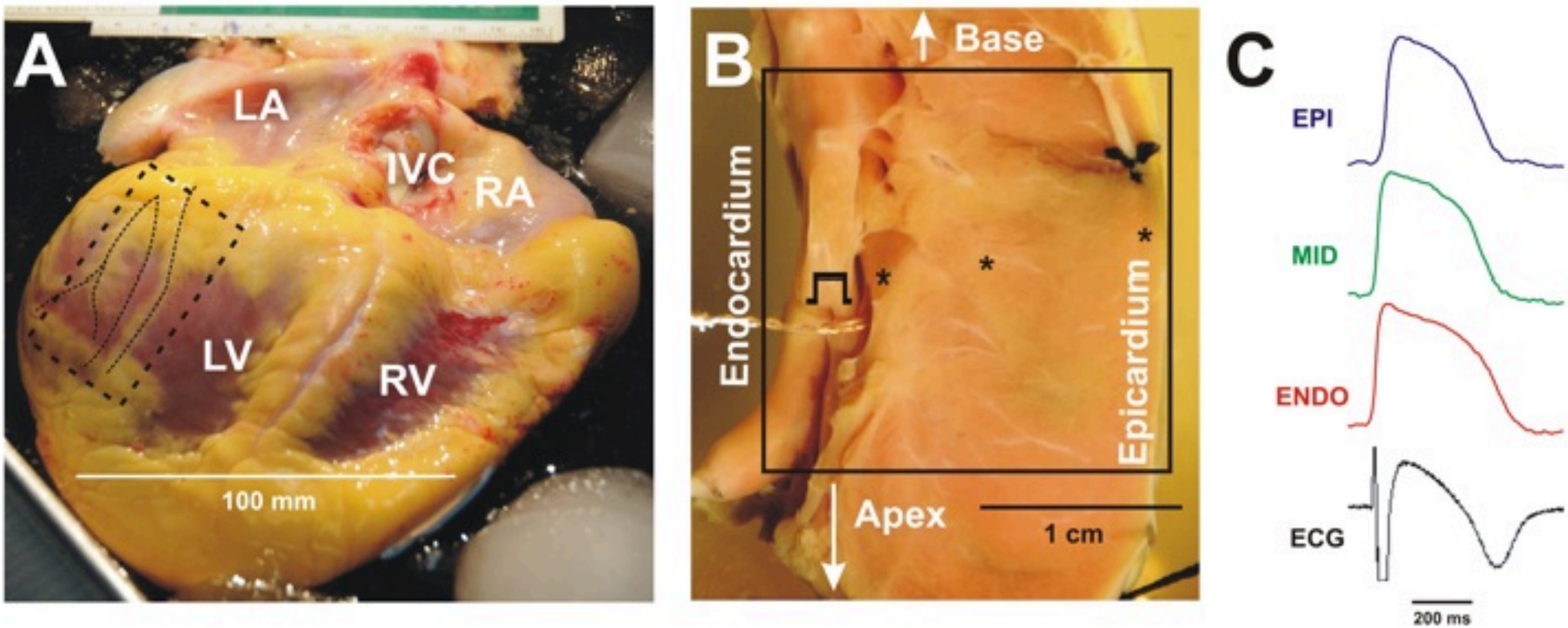

Steep APD Gradient in the "M-cell" region of a non-failing human left ventricle

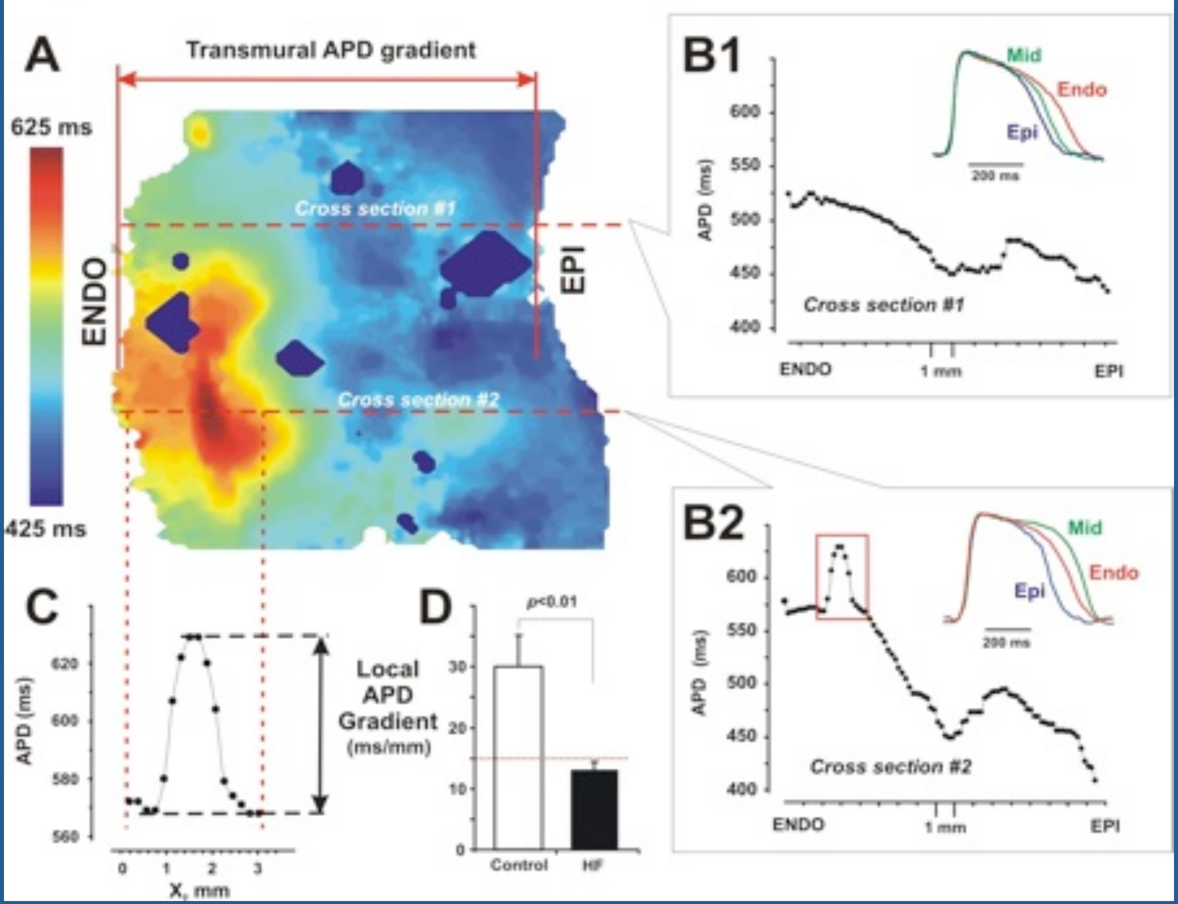

Glukhov, Circ. Res. 2010

Heterogeneity can create spirals

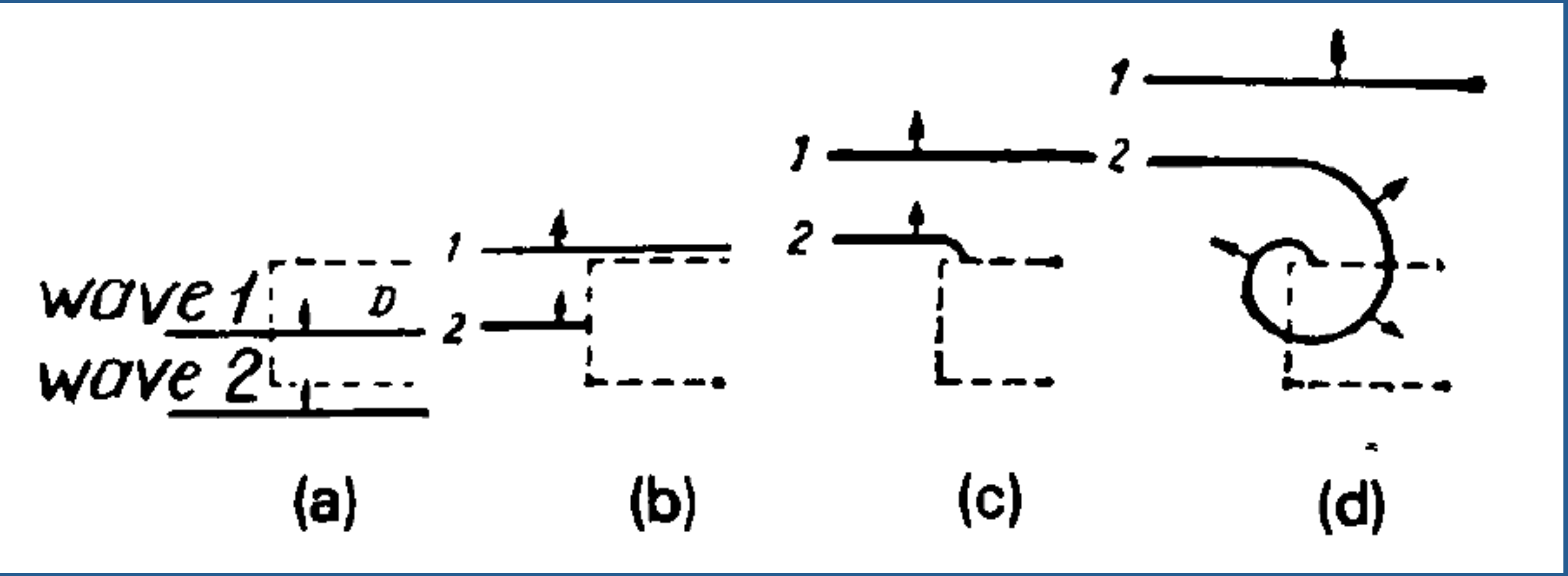

Krinsky 1966

High frequency pacing of a heterogeneity

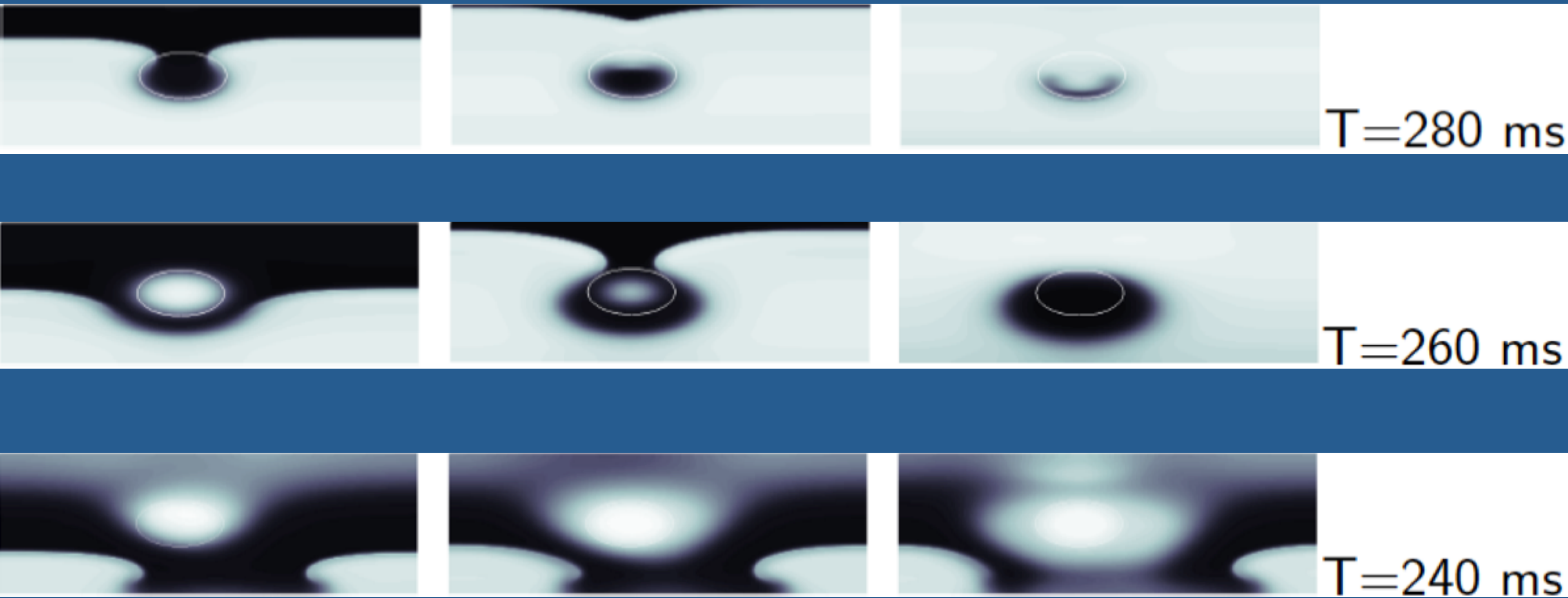

Spiral at a distance from a heterogeneity

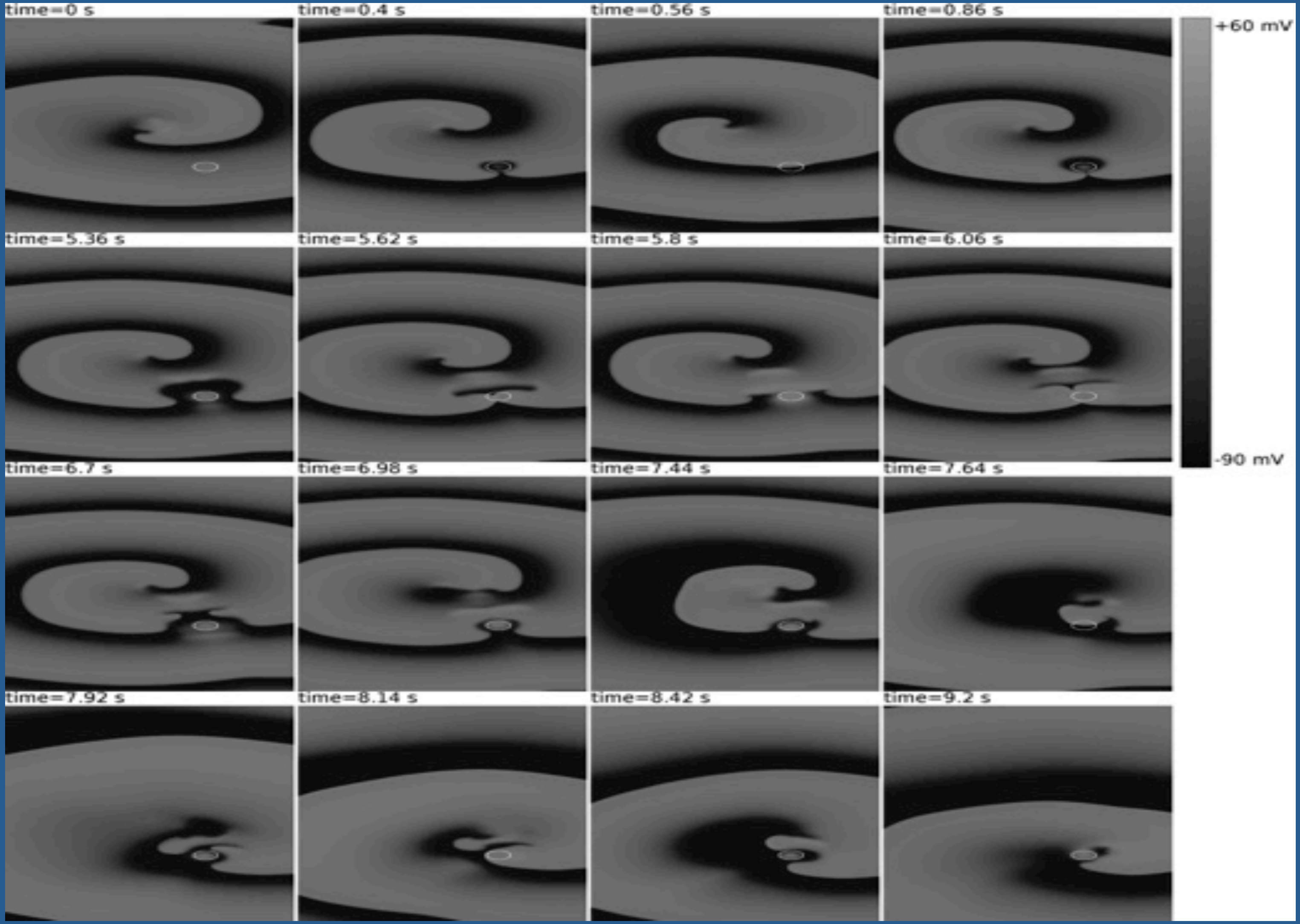

Attraction to an inexcitable obstacle (scar)

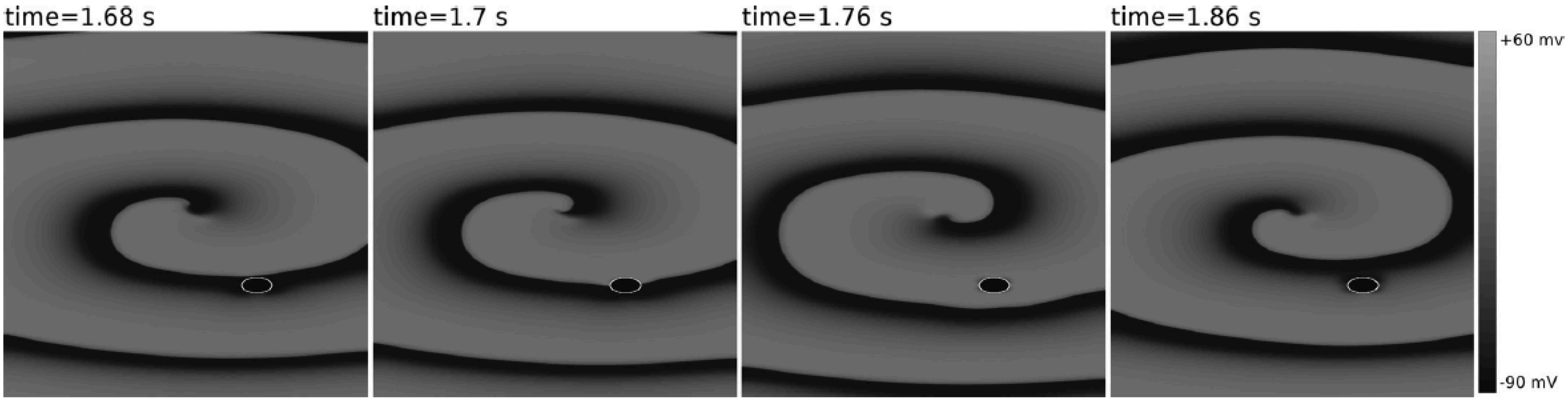

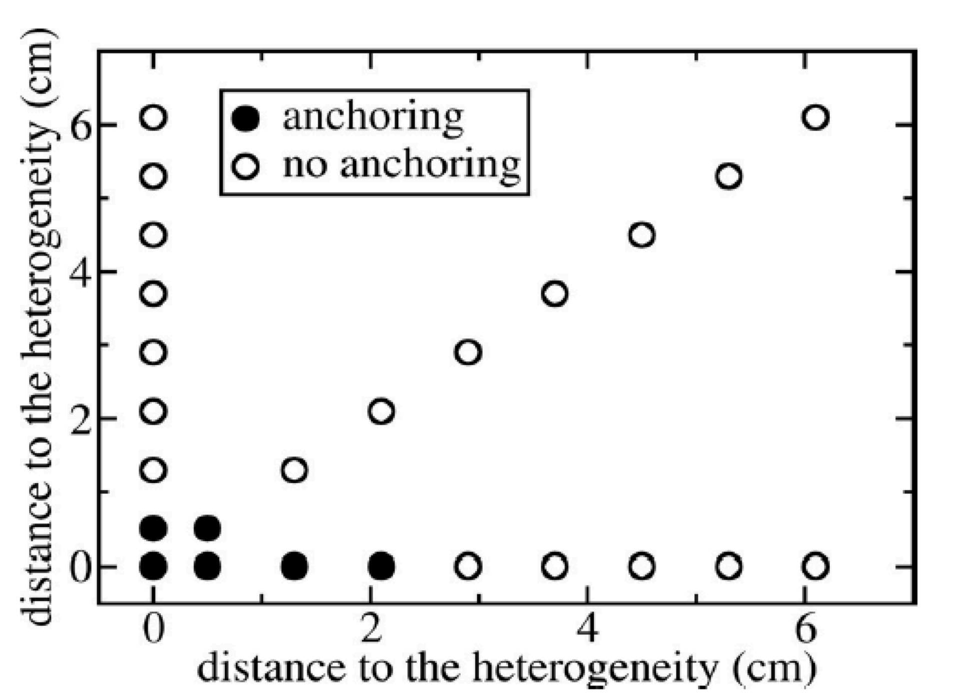

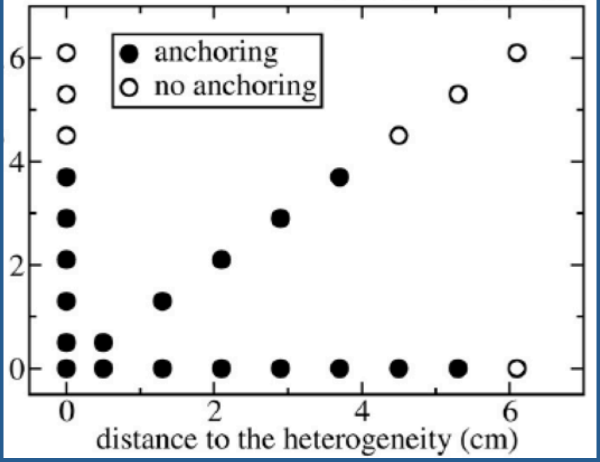

Small size ionic heterogeneities can attract rotors

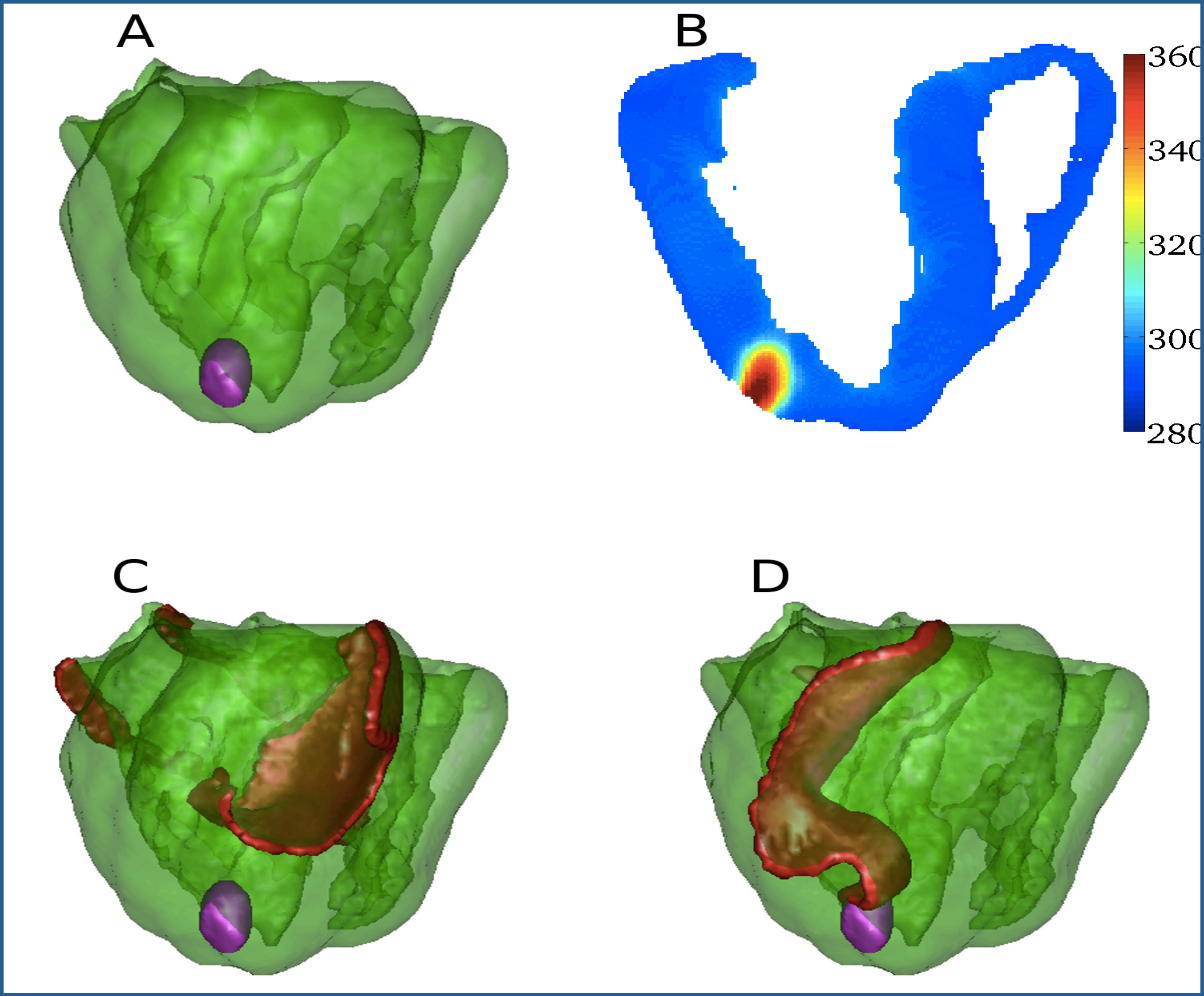

Defauw et al., Am. J. Physiol. 2014

Small size ionic heterogeneities can attract rotors

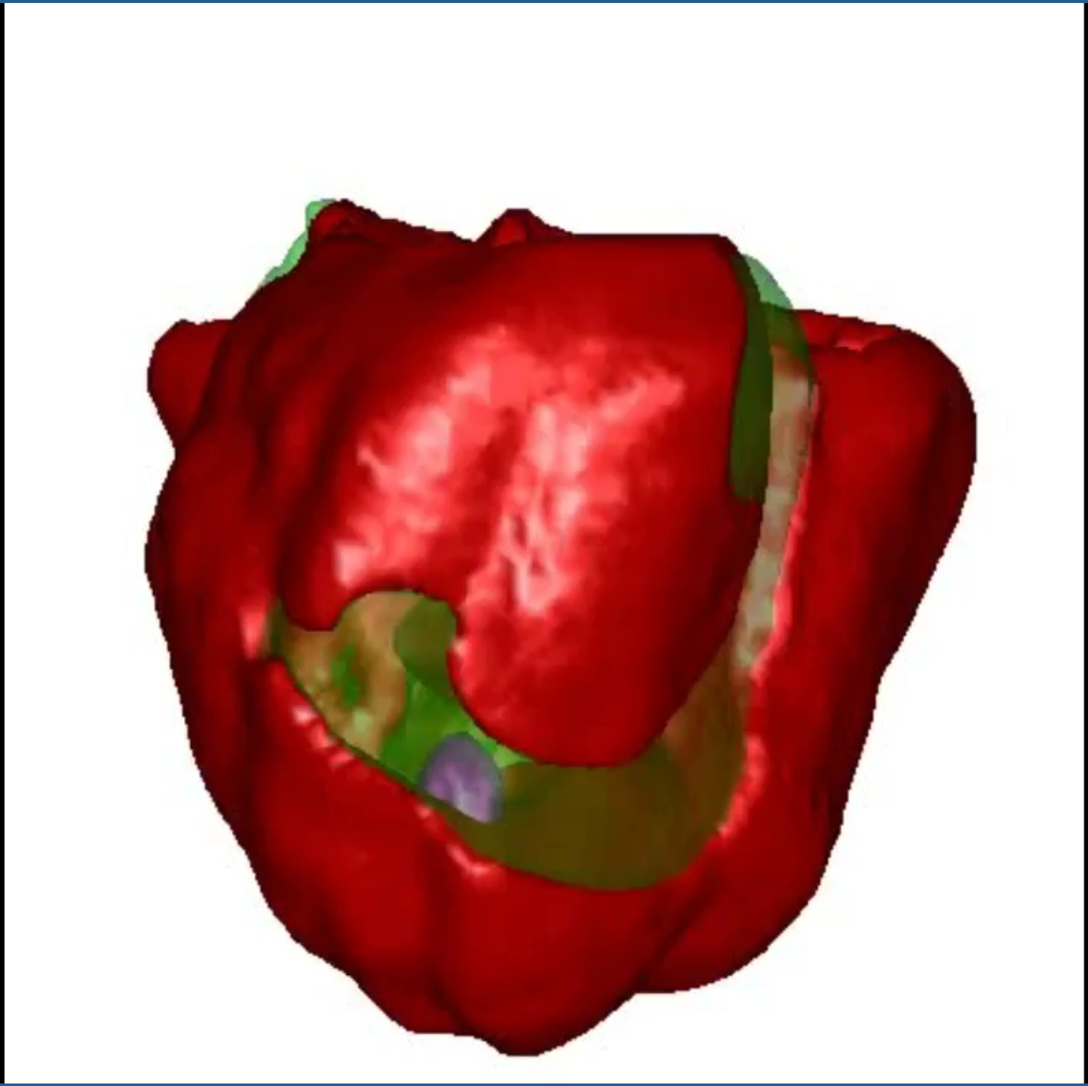

FIBROSIS and ARRHYTHMIAS

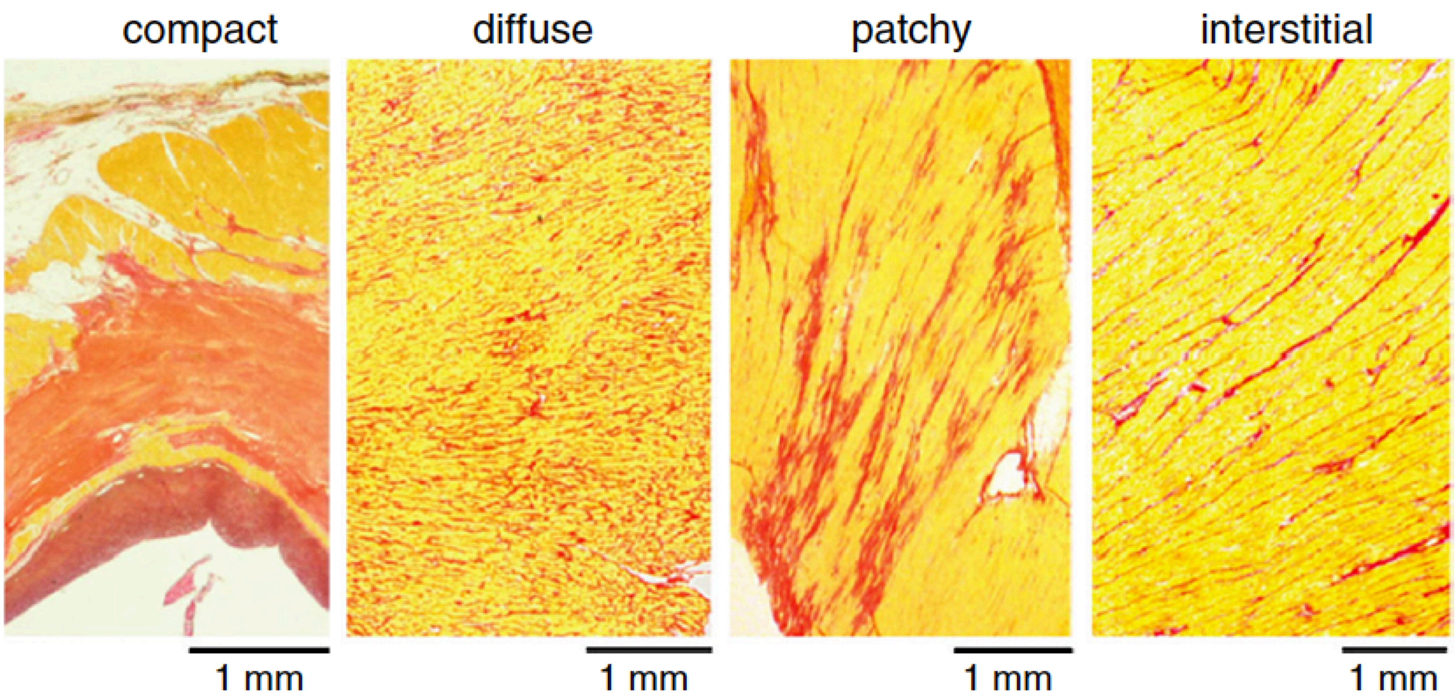

Fig. 1. Cardiac fibrosis patterns influence arrhythmogenic potential. Red = collagen; yellow = myocardium. The most arrhythmogenic patterns are interstitial and patchy, which result in interconnected strands of myocytes separated by collagen bundles.
Modified from de Jong et al. [14] with permission.

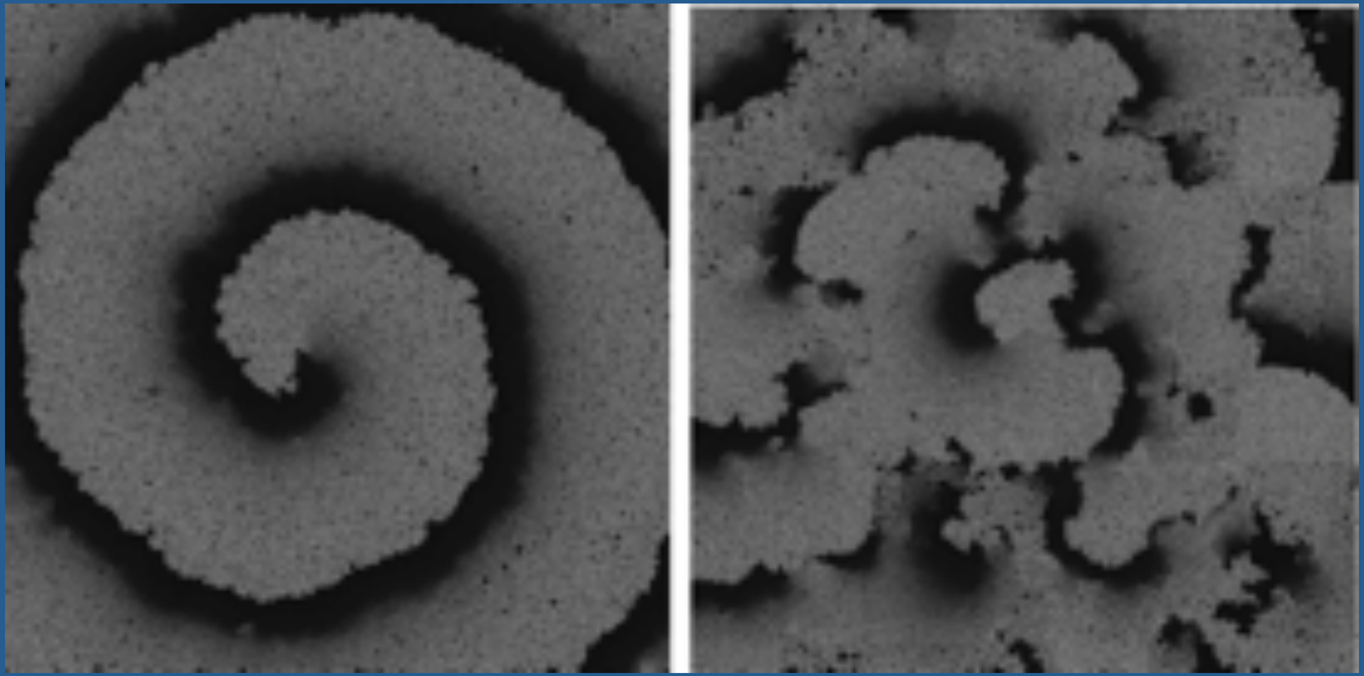

homogeneous heterogeneous

EUROPEAN SOCIETY OF CARDIOLOGY®
European Journal of Heart Failure (2010) **12**, 913–921
doi:10.1093/eurjhf/hfq092

Heterogeneous Connexin43 distribution in heart failure is associated with dispersed conduction and enhanced susceptibility to ventricular arrhythmias

Mohamed Boulaksil[1,2], Stephan K.G. Winckels[2,3], Markus A. Engelen[2,4], Mèra Stein[2,5], Toon A.B. van Veen[2], John A. Jansen[2], André C. Linnenbank[1,6], Marti F.A. Bierhuizen[2], W. Antoinette Groenewegen[2], Matthijs F.M. van Oosterhout[3], Johannes H. Kirkels[5], Nicolaas de Jonge[5], András Varró[7,8], Marc A. Vos[2], Jacques M.T. de Bakker[1,2,6], and Harold V.M. van Rijen[2*]

Methods and results Clinical and (immuno)histological data of myocardial biopsies from CHF patients with (VT+) and without (VT−) documented ventricular arrhythmia were compared with controls. In CHF patients, ejection fraction was decreased and QRS duration was increased. Cell size and interstitial fibrosis were increased, but Connexin43 (Cx43) levels, the most abundant gap junction in ventricular myocardium, were unchanged. No differences were found between VT+ and VT− patients, except for the distribution pattern of Cx43, which was significantly more heterogeneous in VT+. Mice were subjected to transverse aortic constriction (TAC) or sham operated. At 16 weeks, cardiac function was determined by echocardiography and epicardial ventricular activation mapping was performed. Transverse aortic constriction mice had decreased fractional shortening and prolonged QRS duration. Right ventricular conduction velocity was reduced, and polymorphic VTs were induced in 44% TAC and 0% sham mice. Interstitial fibrosis was increased and Cx43 quantity was unchanged in TAC mice with and without arrhythmias. Similar to CHF patients, heterogeneous Cx43 distribution was significantly associated with arrhythmias in TAC mice and with spatial heterogeneity of impulse conduction.

Conclusion Heterogeneous Cx43 expression during CHF is associated with dispersed impulse conduction and may underlie enhanced susceptibility to ventricular tachyarrhythmias.

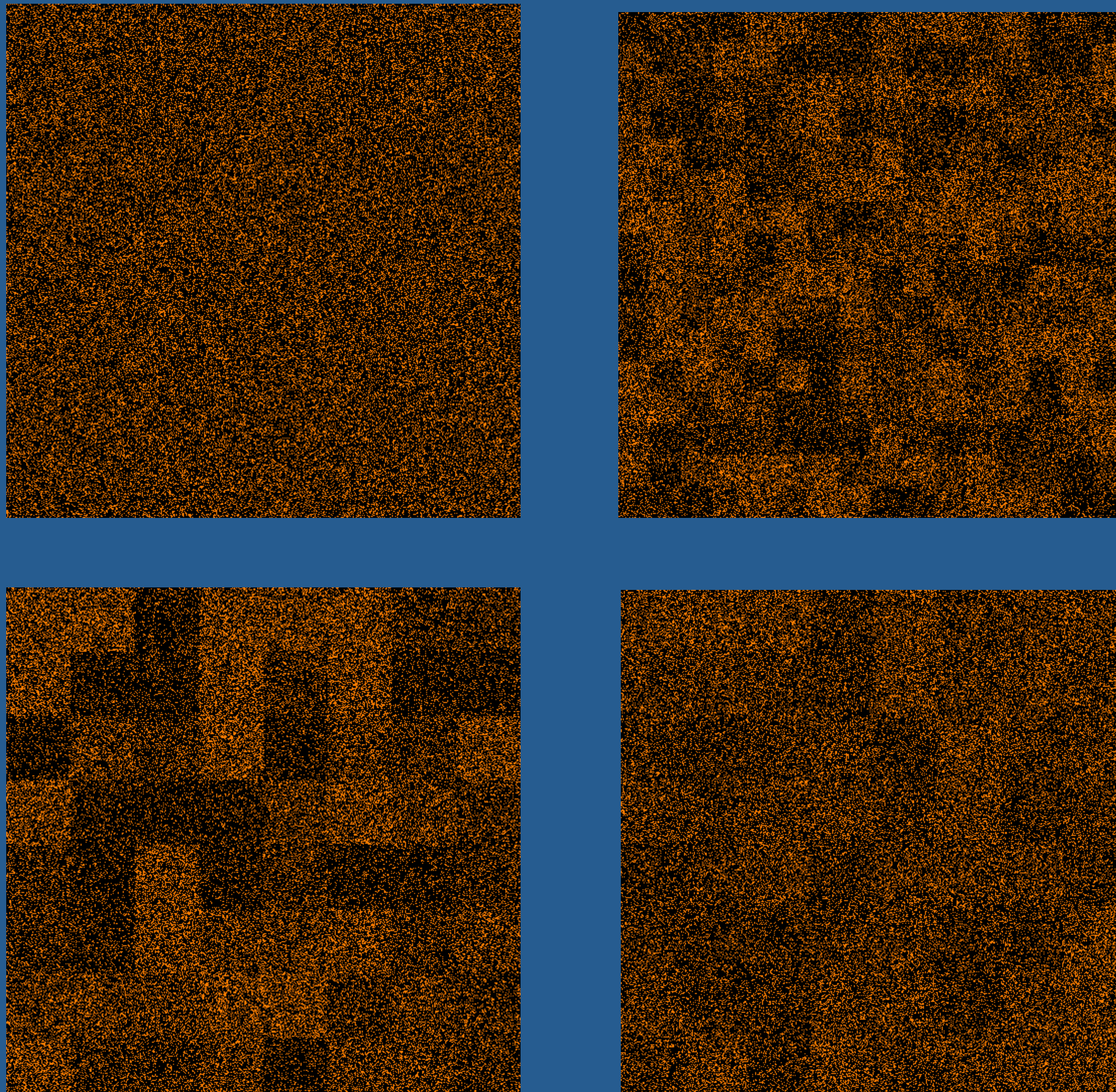

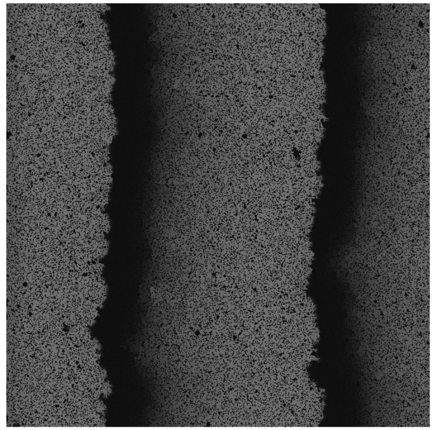

$t = 2.3$ s

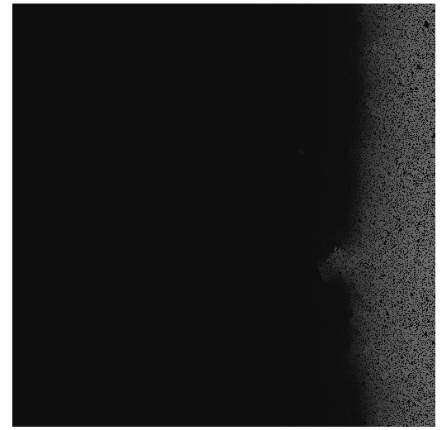

$t = 2.7$ s

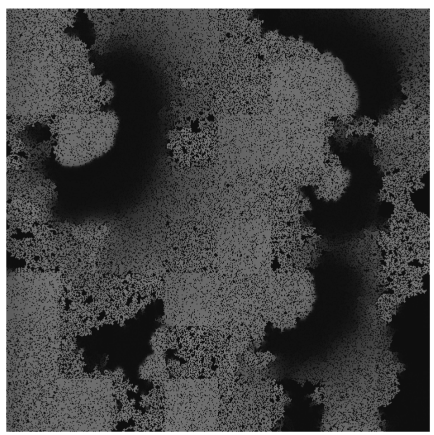

$t = 2.3$ s

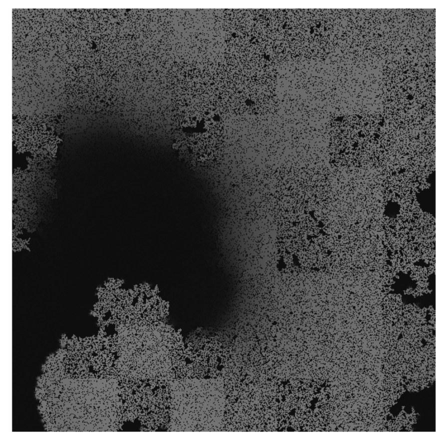

$t = 3.1$ s

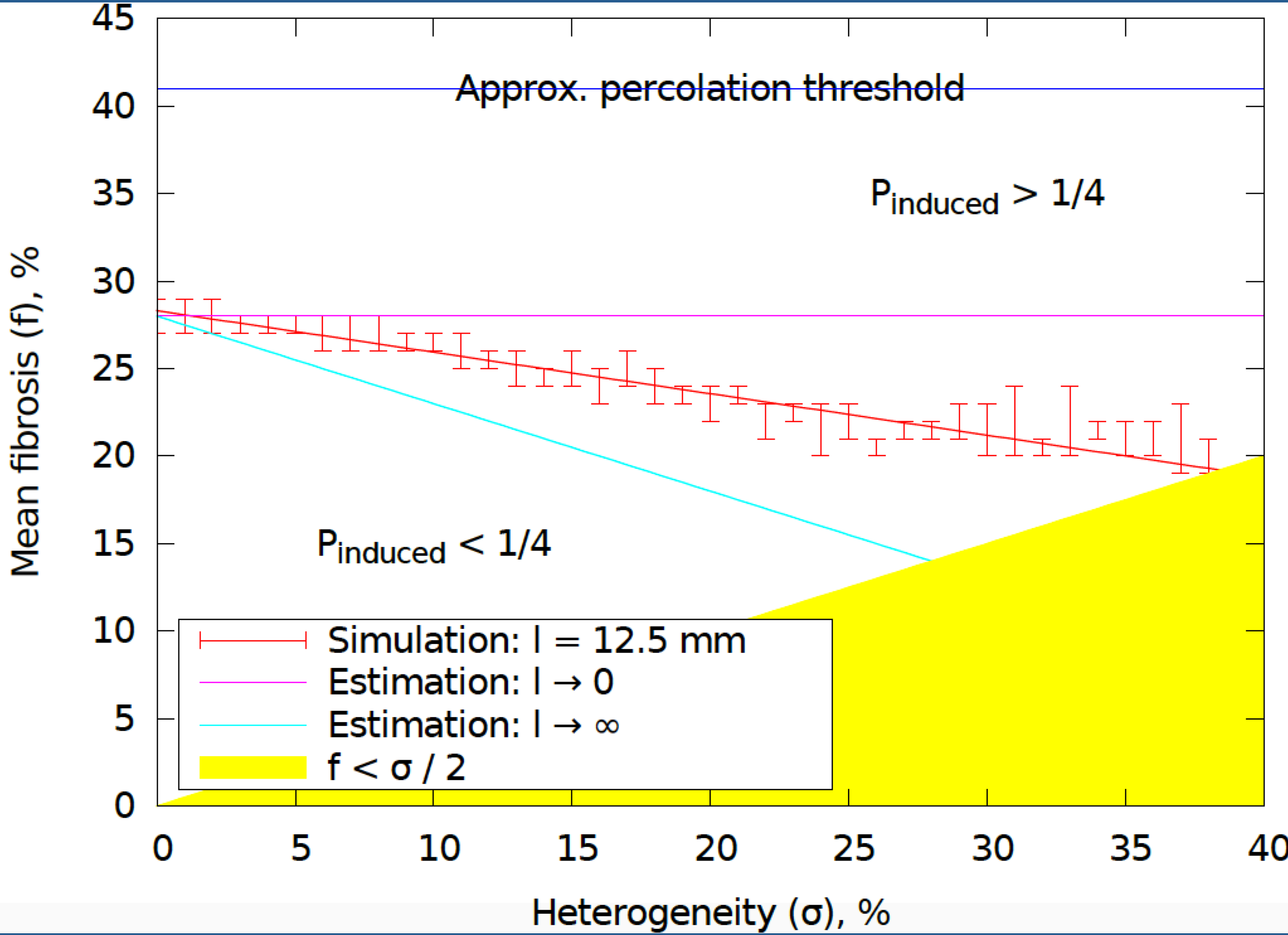

Approx. percolation threshold
$P_{induced} > 1/4$
$P_{induced} < 1/4$
Simulation: l = 12.5 mm
Estimation: l → 0
Estimation: l → ∞
f < σ / 2
Mean fibrosis (f), %
Heterogeneity (σ), %
0
5
10
15
20
25
30
35
40
45

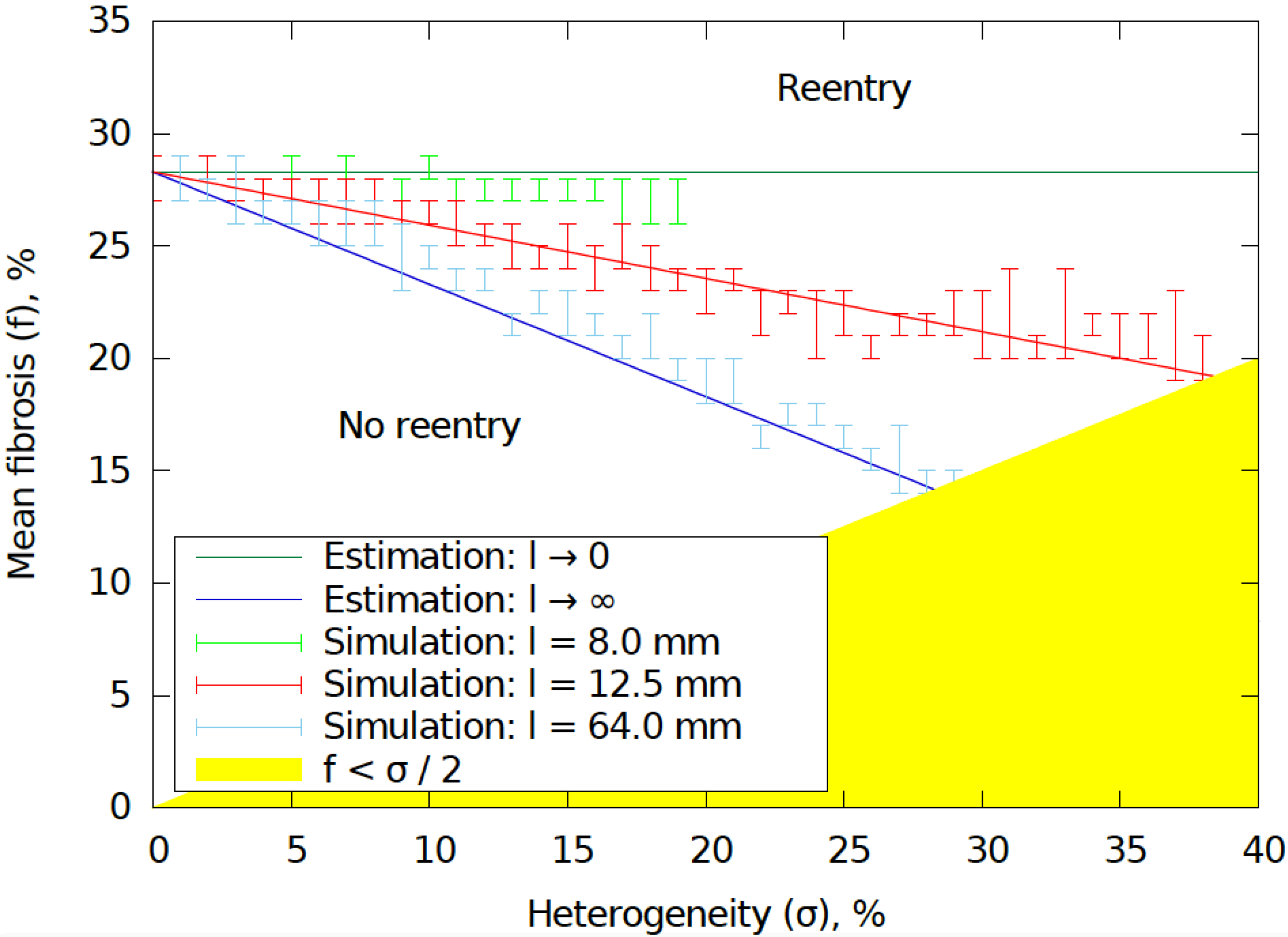

Reentry
No reentry
Estimation: l → 0
Estimation: l → ∞
Simulation: l = 8.0 mm
Simulation: l = 12.5 mm
Simulation: l = 64.0 mm
f < σ / 2
Mean fibrosis (f), %
Heterogeneity (σ), %
0
5
10
15
20
25
30
35
40

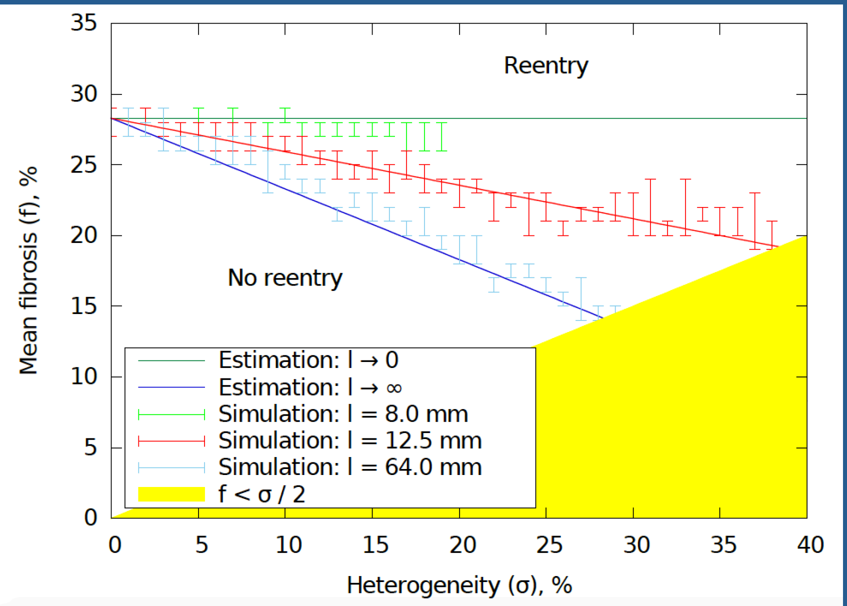

Heterogeneity σ means fibrosis percentage is $f-\sigma/2<\text{fibrosis}<f+\sigma/2$ where f is mean fibrosis σ is heterogeneity

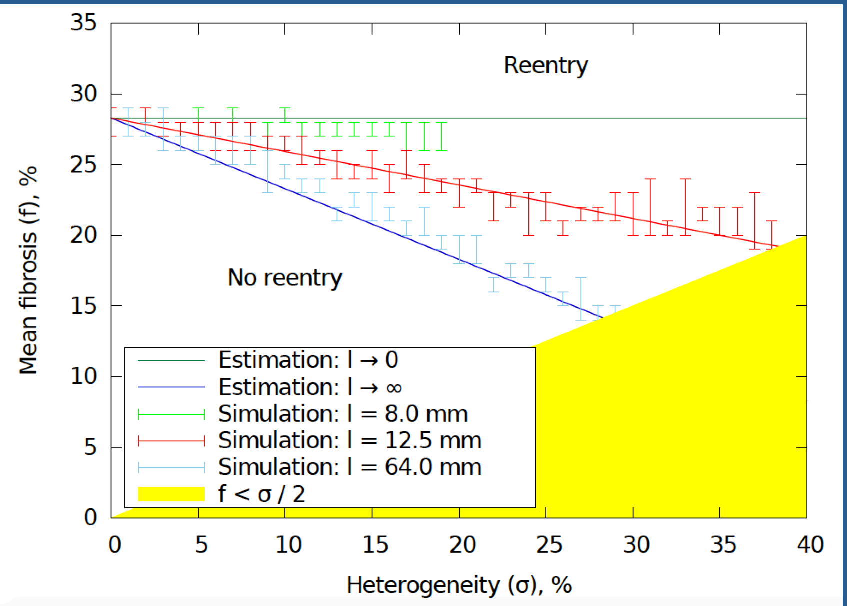

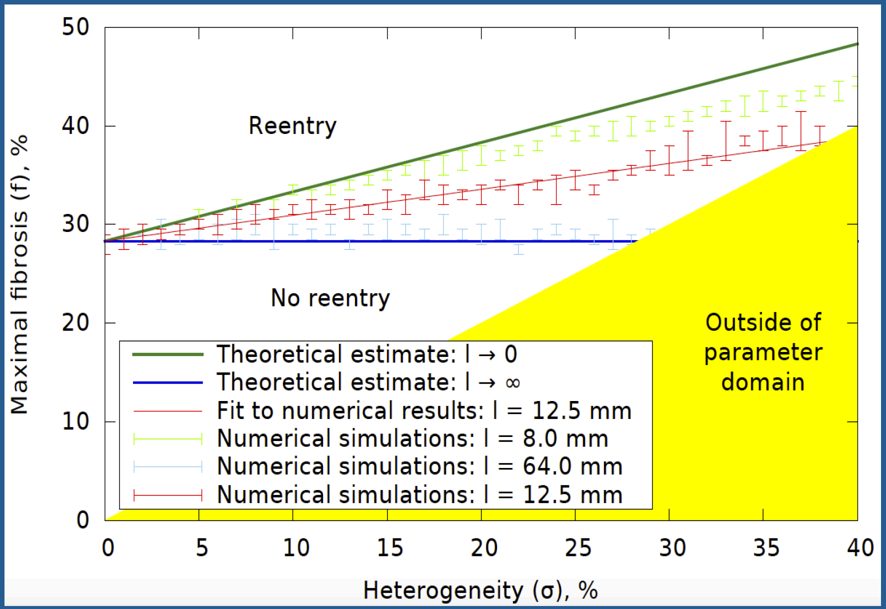

Heterogeneity σ means fibrosis percentage is

f-σ/2<fibrosis <f+σ/2

where f is mean fibrosis

σ is heterogeneity

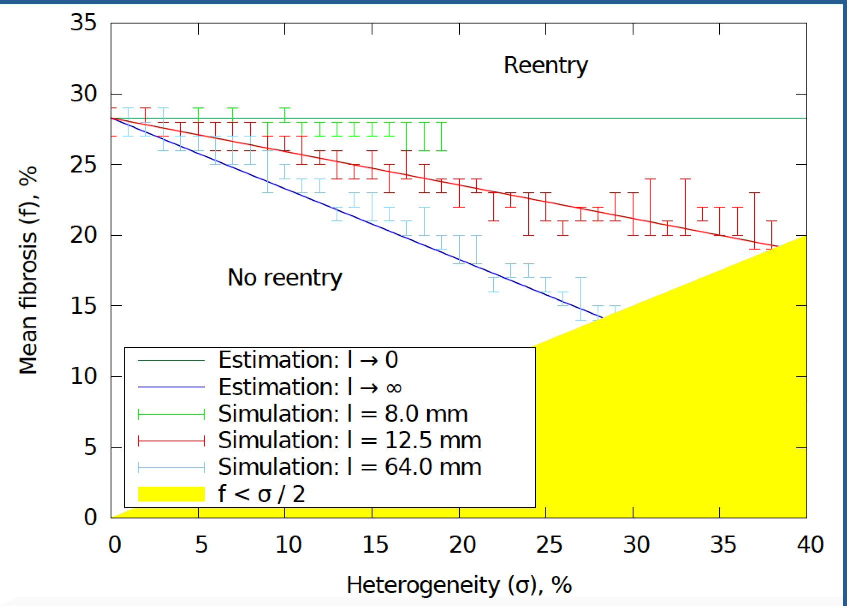

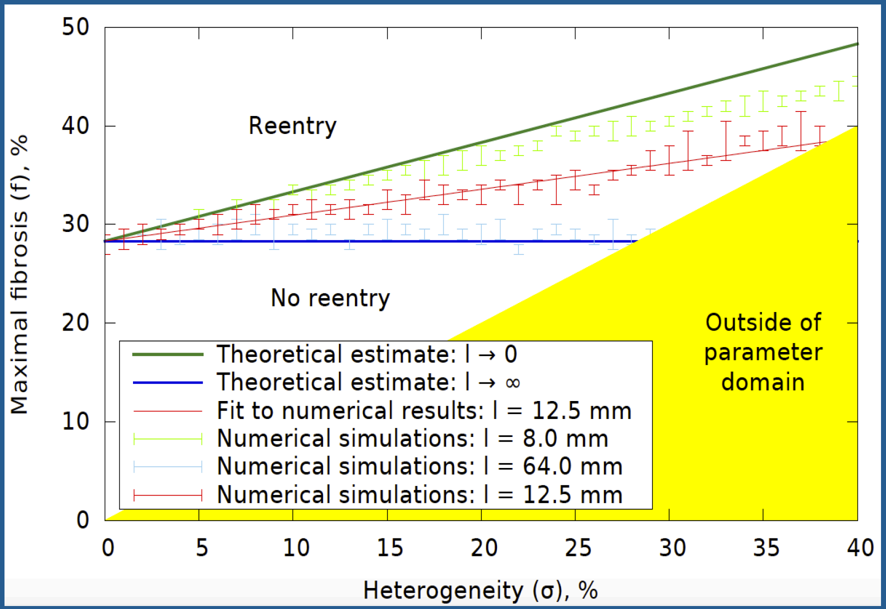

Heterogeneity σ means
fibrosis percentage is
f-σ/2<fibrosis <f+σ/2
where f is mean fibrosis
σ is heterogeneity

ALL IS DETERMMINED BY REGIONS WITH LARGEST FIBROSIS

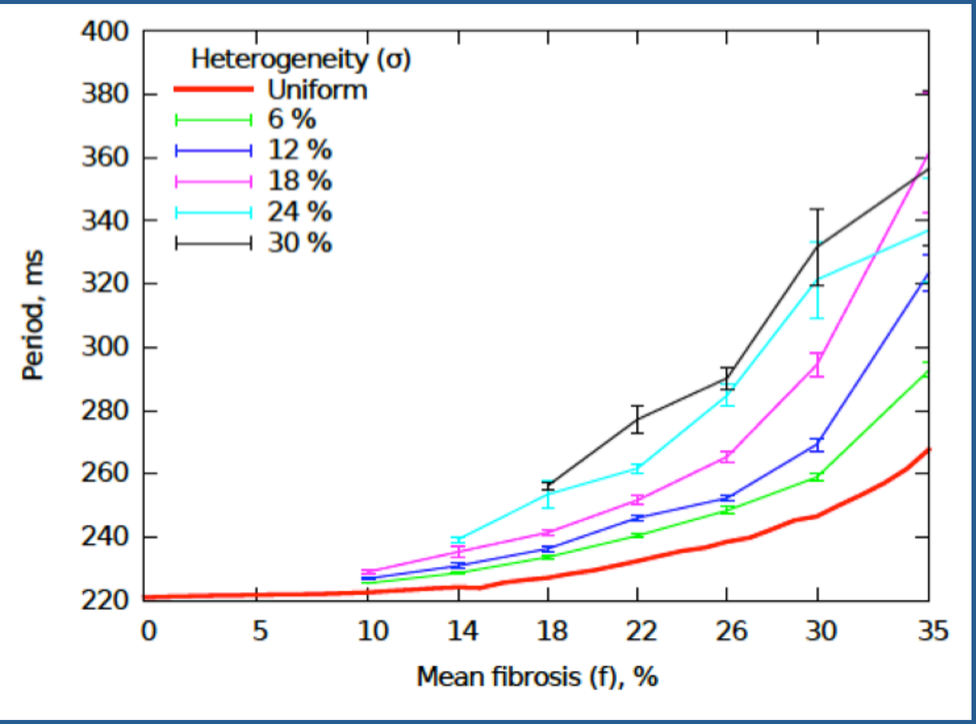

dependency of the period on the mean fibrosis for different values of heterogeneity when l = 16 mm.

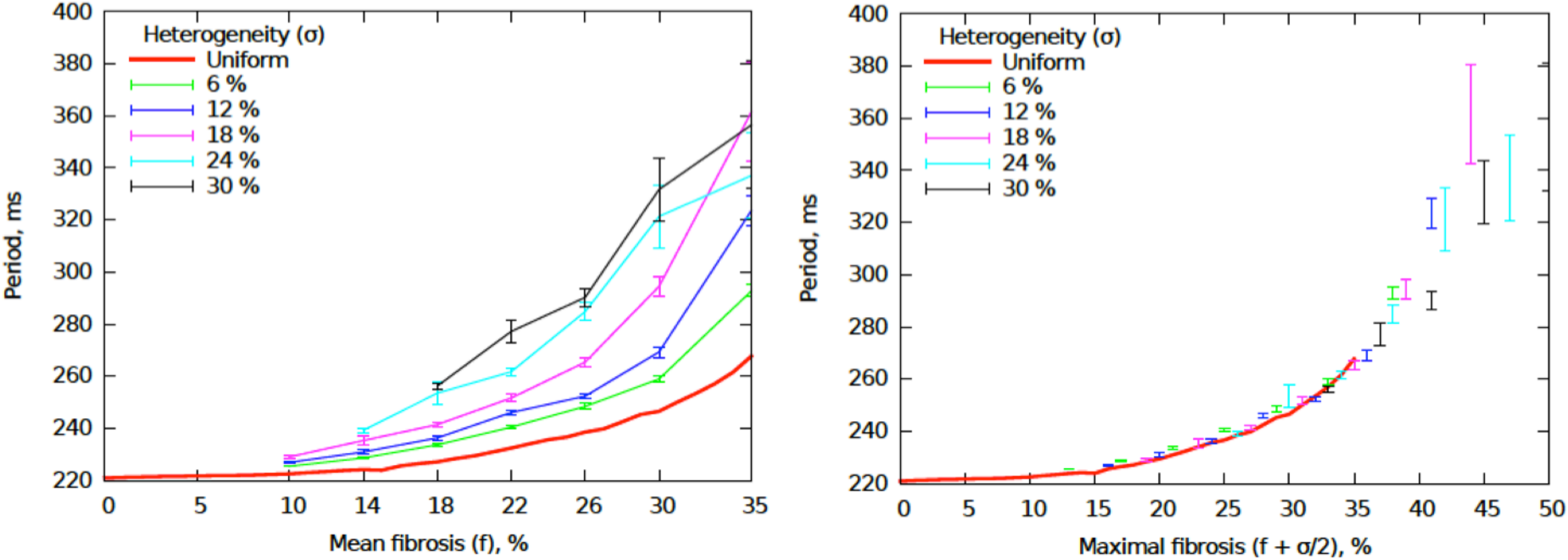

Heterogeneity (σ)
Uniform
6 %
12 %
18 %
24 %
30 %
Period, ms
Mean fibrosis (f), %
Maximal fibrosis (f + σ/2), %
400
380
360
340
320
300
280
260
240
220
0
5
10
14
18
22
26
30
35
15
20
25
40
45
50

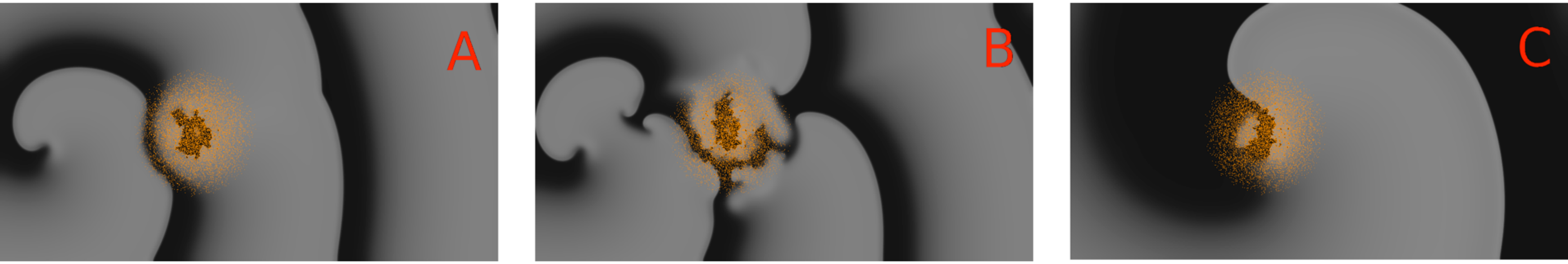

Fig. 1: Spiral wave anchoring to a fibrotic region in the 2D model. Inexcitable fibrotic tissue is shown with orange and the transmembrane voltage is shown in shades of gray. A: A spiral wave initiated 4.3 cm away from the border of the fibrotic region (t = 0 s). B: The wavefront breaks on the fibrotic region and some secondary sources propagate towards the tip of the spiral wave (t = 4.8 s). C: One of the secondary sources merged with the tip of the spiral. This restructuring of the activation pattern resulted in emergence of a single spiral wave anchored to the scar.

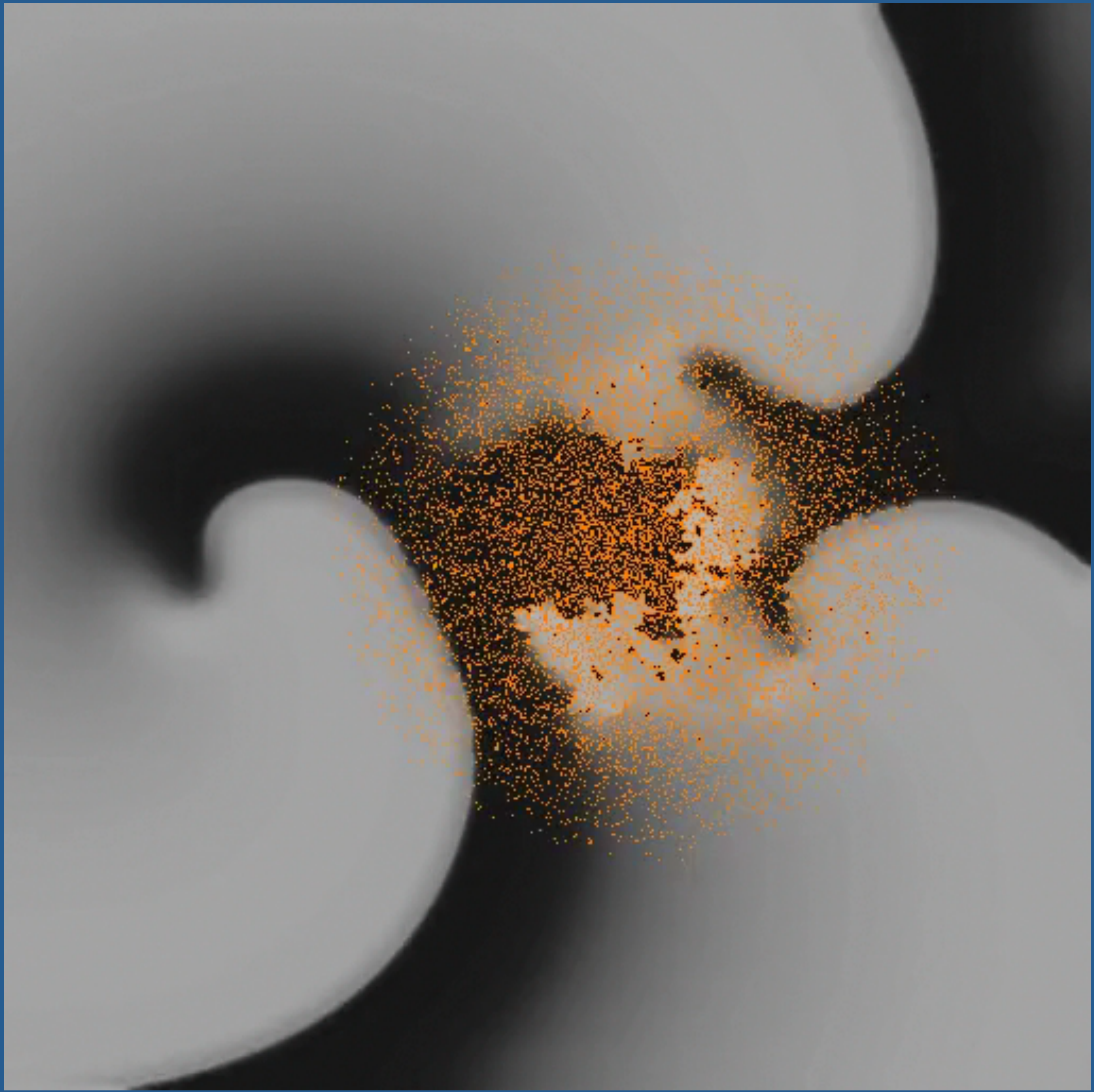

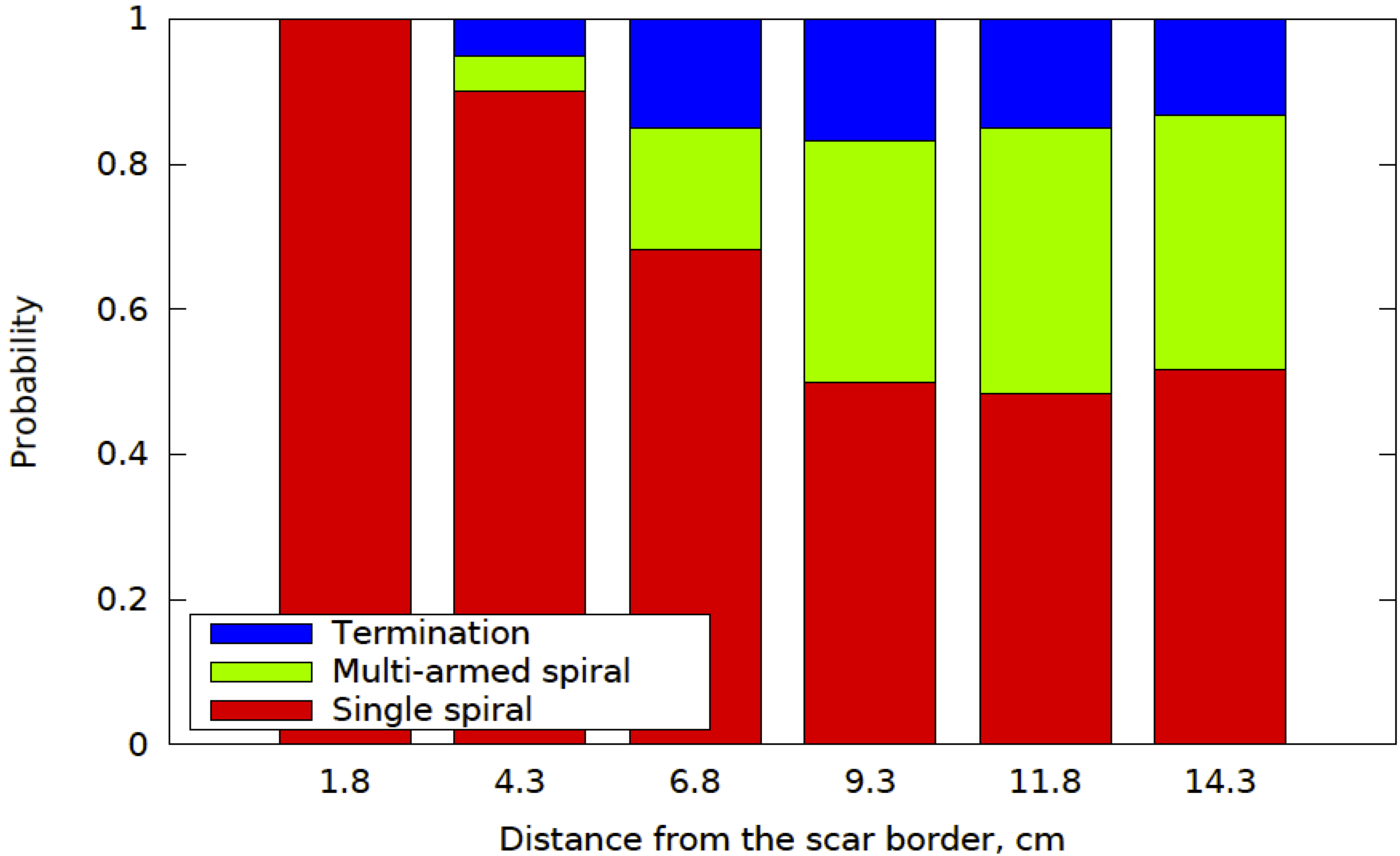
Probability
1
0.8
0.6
0.4
0.2
0
Termination
Multi-armed spiral
Single spiral
1.8
4.3
6.8
9.3
11.8
14.3
Distance from the scar border, cm

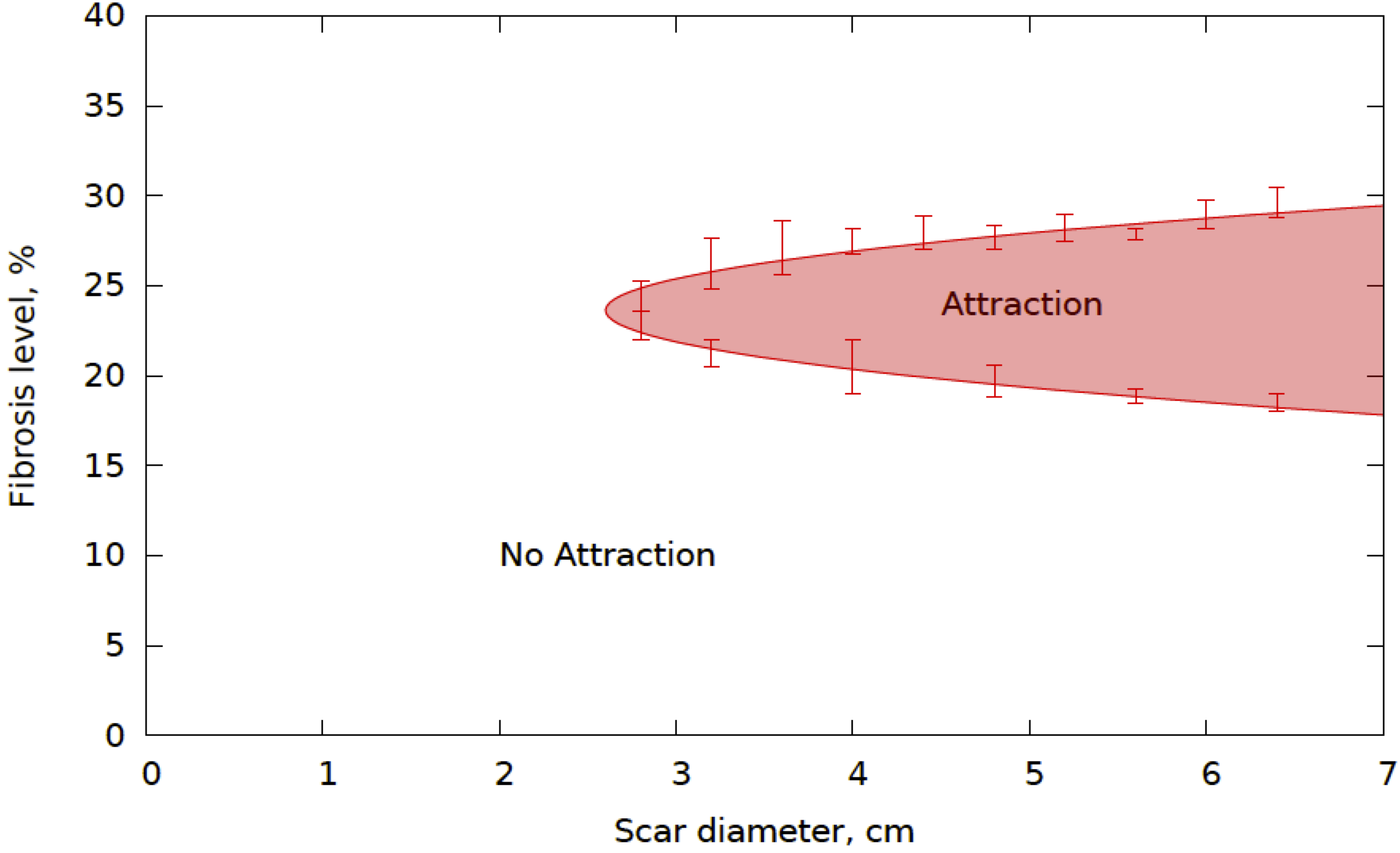

Attraction
No Attraction
Fibrosis level, %
Scar diameter, cm
40
35
30
25
20
15
10
5
0
0
1
2
3
4
5
6
7

MRI heart data

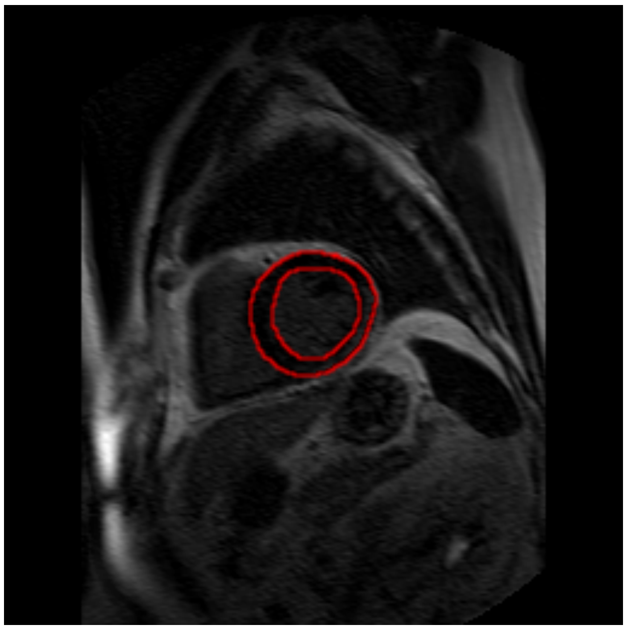

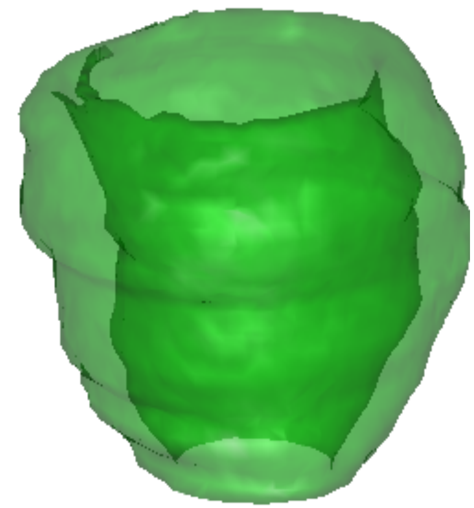

Original image

Segmented LV

Reconstruction

Generation of fibers

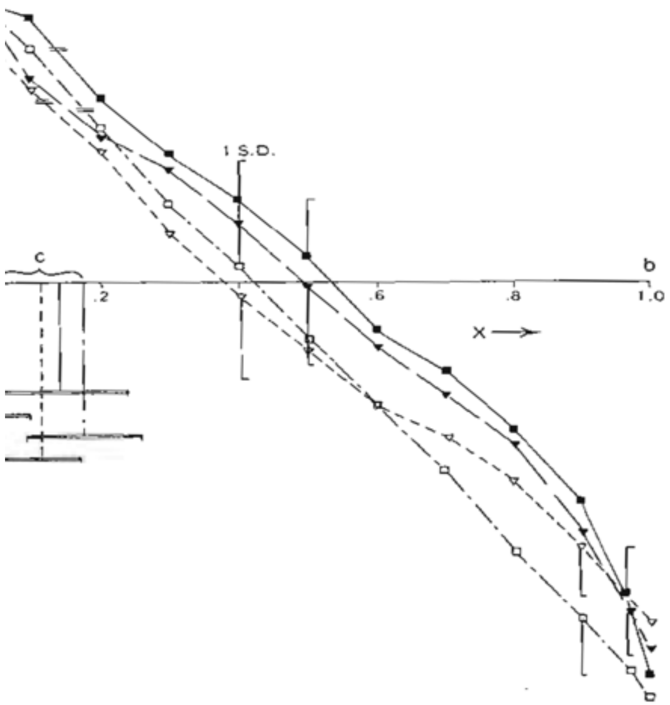

$$|\nabla u| = 1$$

$$u_{epi} : u(x) = 0, x \in Epicardium$$

$$u_{endo} : u(x) = 0, x \in Endocardium$$

$$b = \frac{u_{endo}}{u_{epi} + u_{endo}}$$

$$\alpha_1 = 50 + (-70 - 50)\, b$$

Streeter (1979): through-wall distribution of helix angle for human left ventricle

Generation of fibers

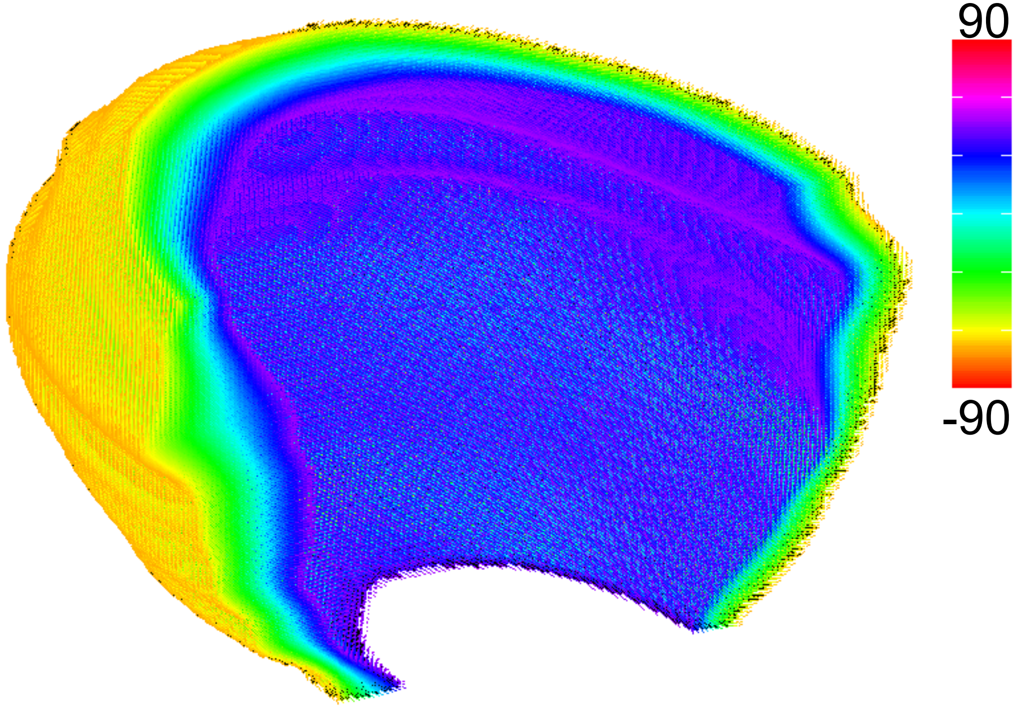

Fibrosis

Gray level corresponds to the ratio of inexcitable tissue

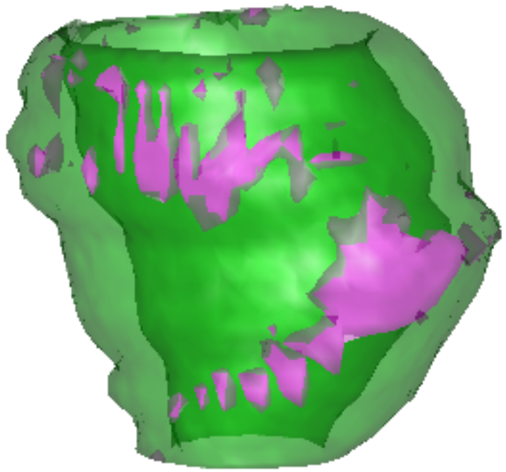

Reconstructed heart with the scar

This was modeled with small inexcitable obstacles

In presence of fibrosis

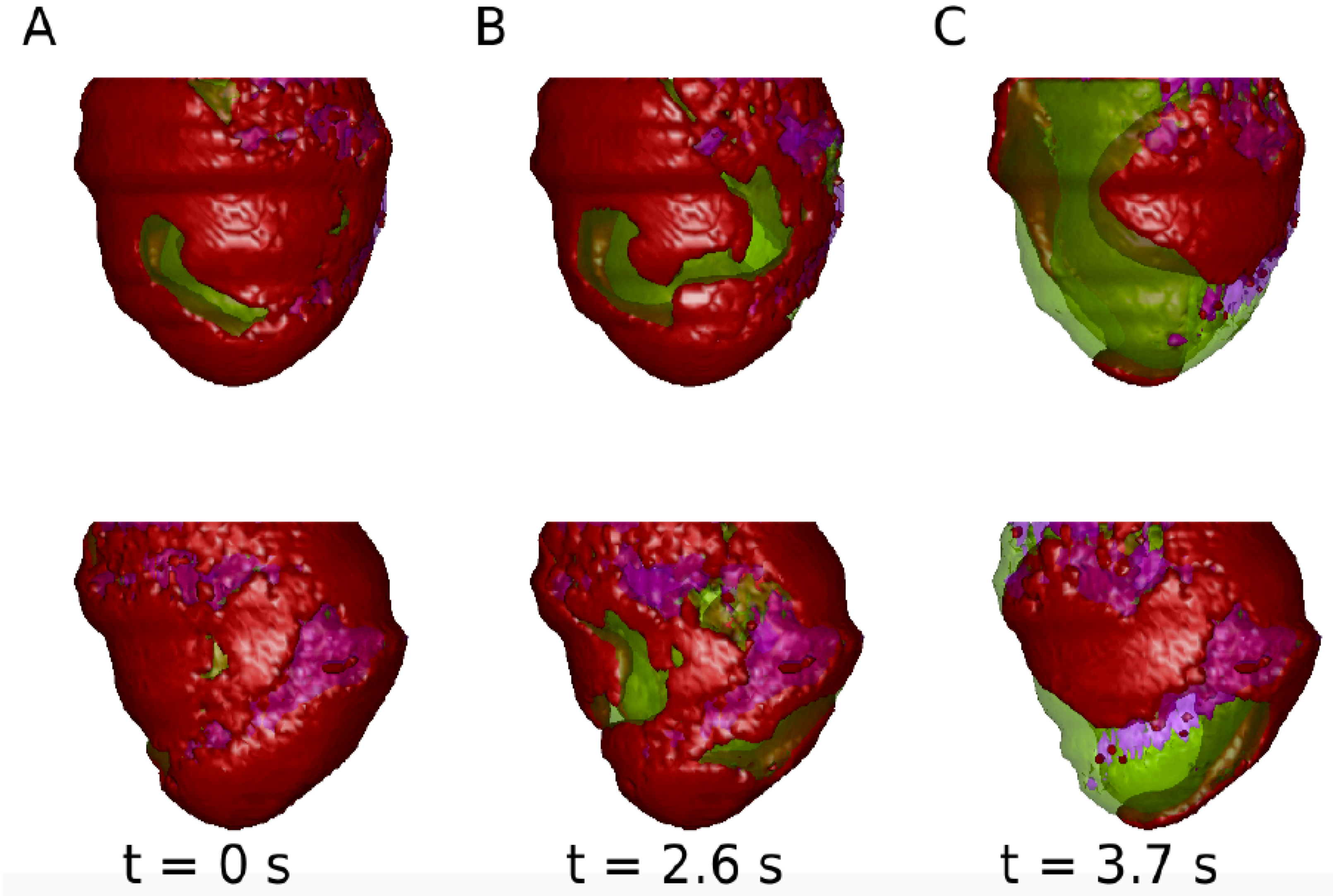

Kazbanov, Vandersickel et al., (in preparation)

In presence of fibrosis

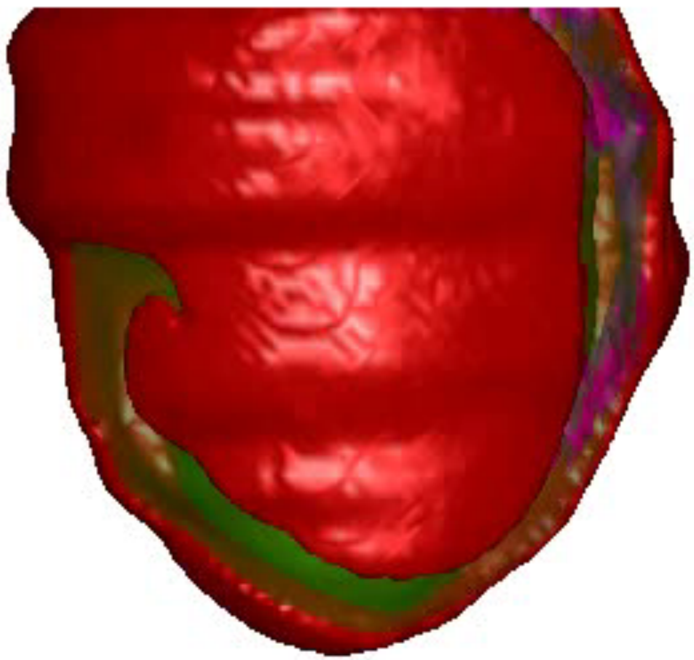

Kazbanov, Vandersickel et al., (in preparation)

In presence of fibrosis

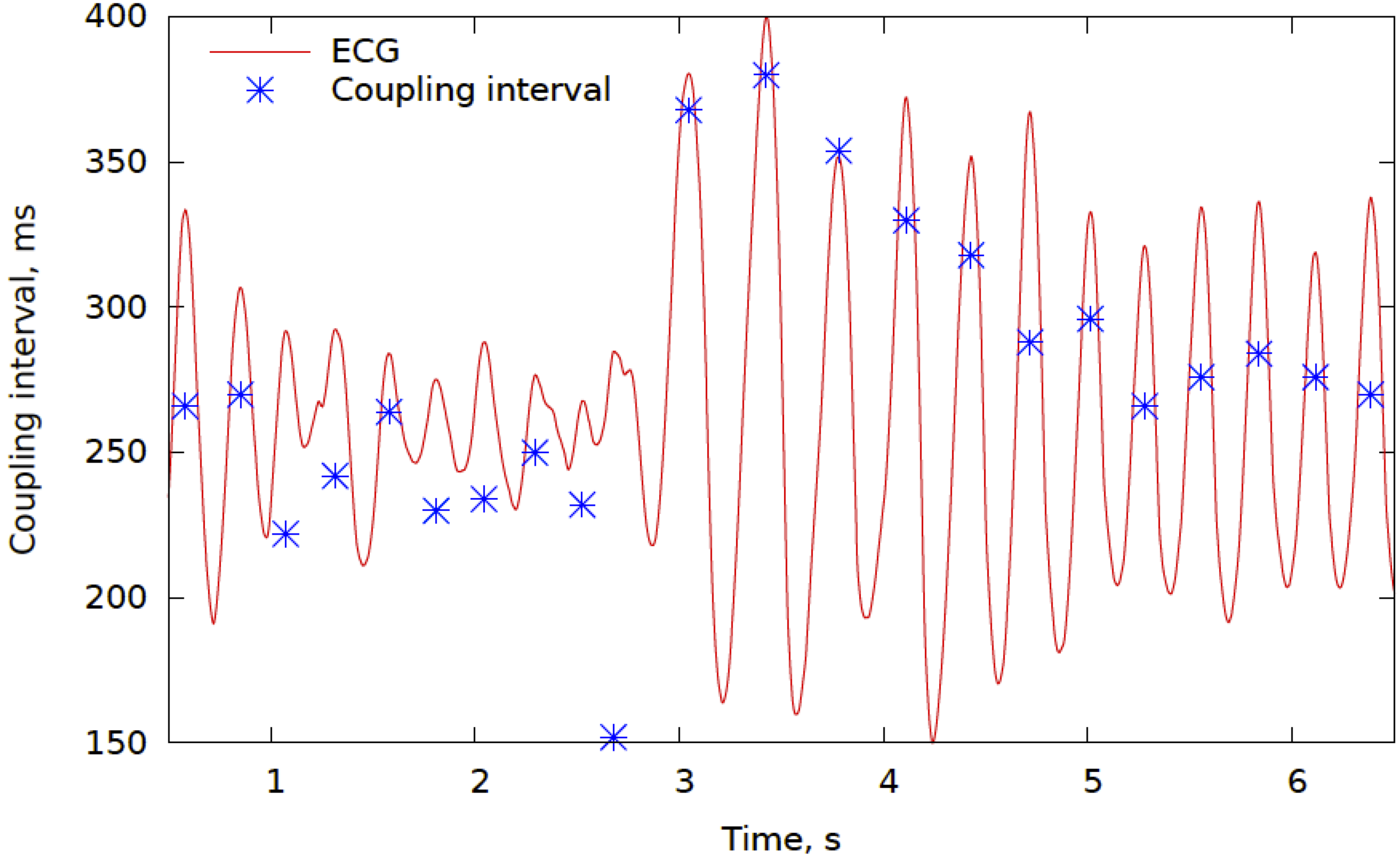

Kazbanov, Vandersickel et al., (in preparation)

In presence of fibrosis

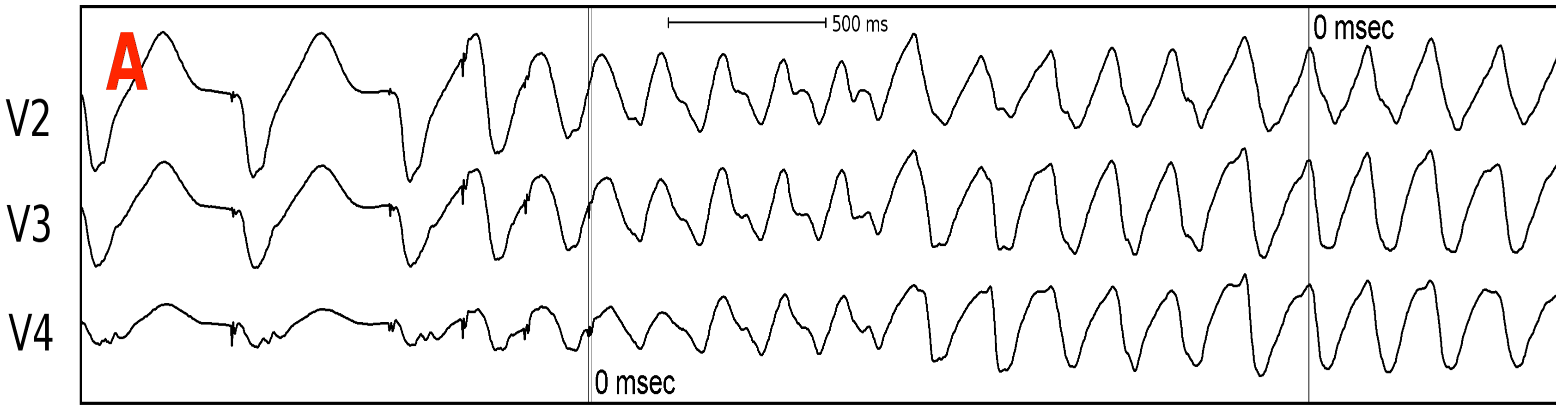

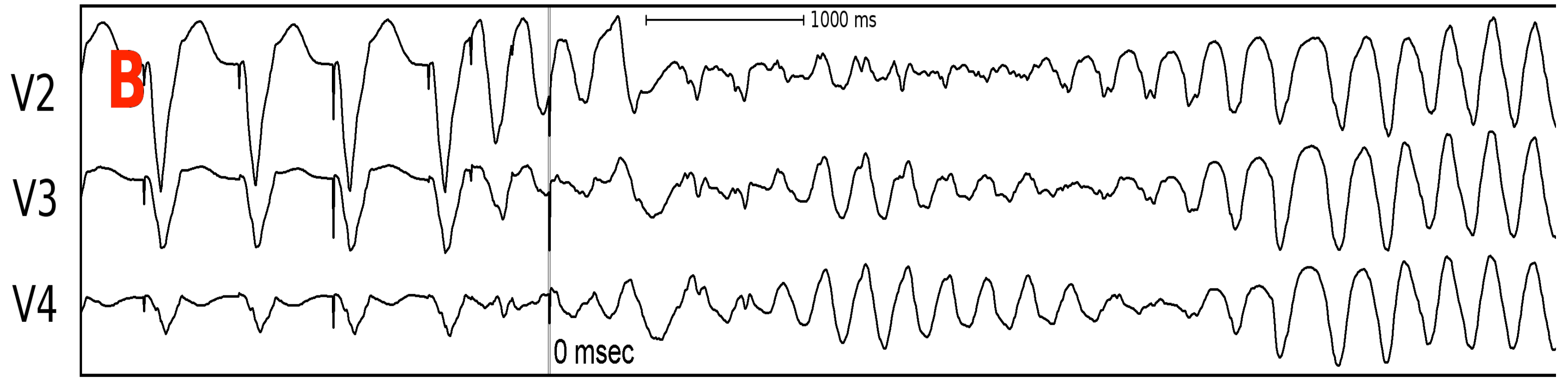

Leads V2, V3, and V4 of clinical ECGs obtained during incuction of ventricular tachicardia for two patients with scars in the left ventricle. First several beats until the mark "0 msec" correspond to external pacing.

Kazbanov, Vandersickel et al., (in preparation)

Global alernans instability

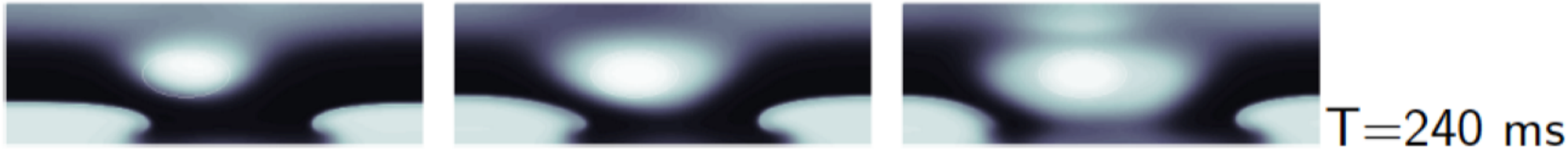

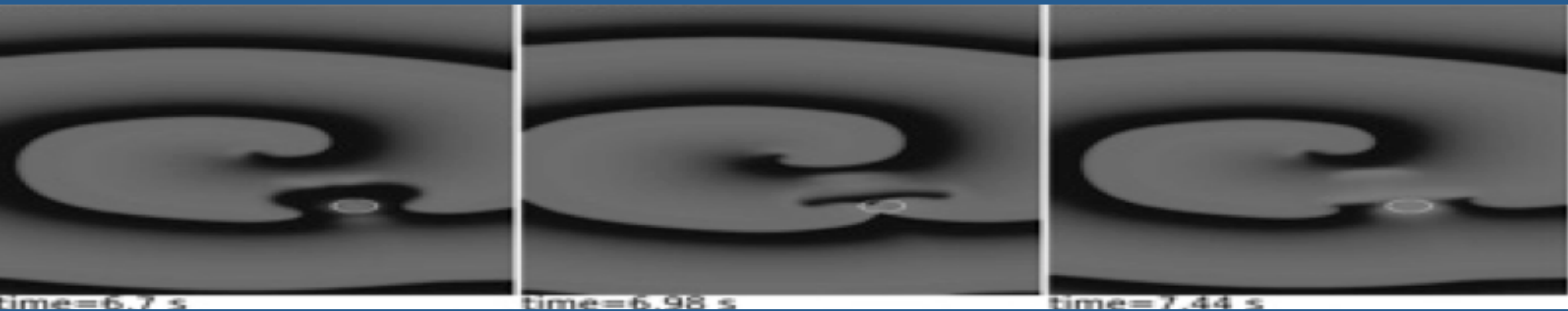

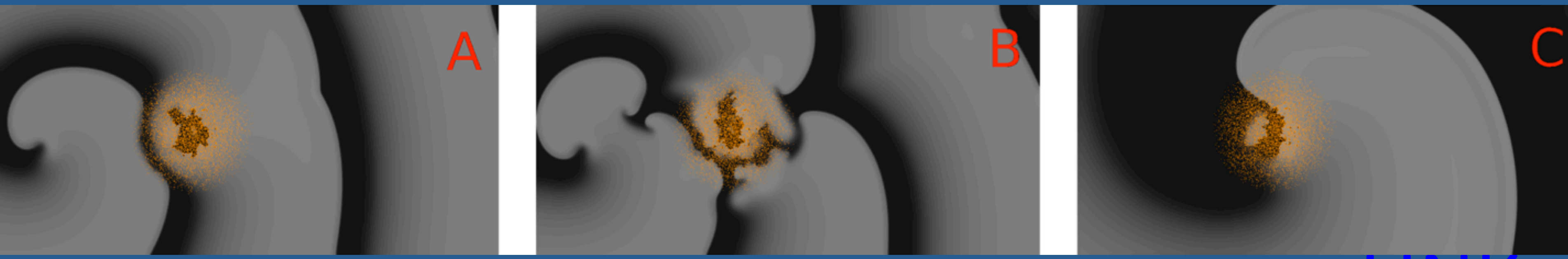

LINK

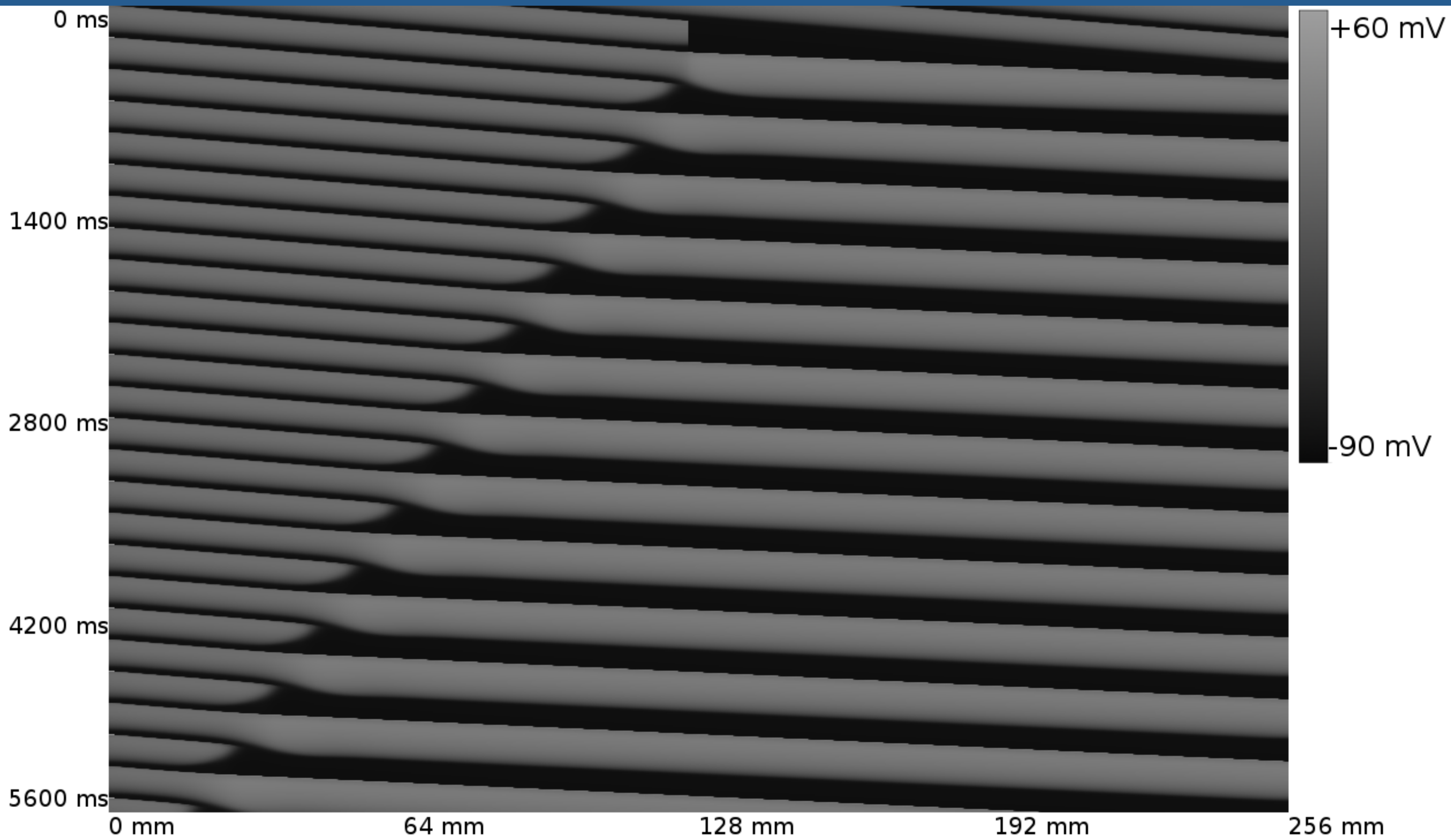

0 ms
1400 ms
2800 ms
4200 ms
5600 ms
0 mm
64 mm
128 mm
192 mm
256 mm
+60 mV
-90 mV

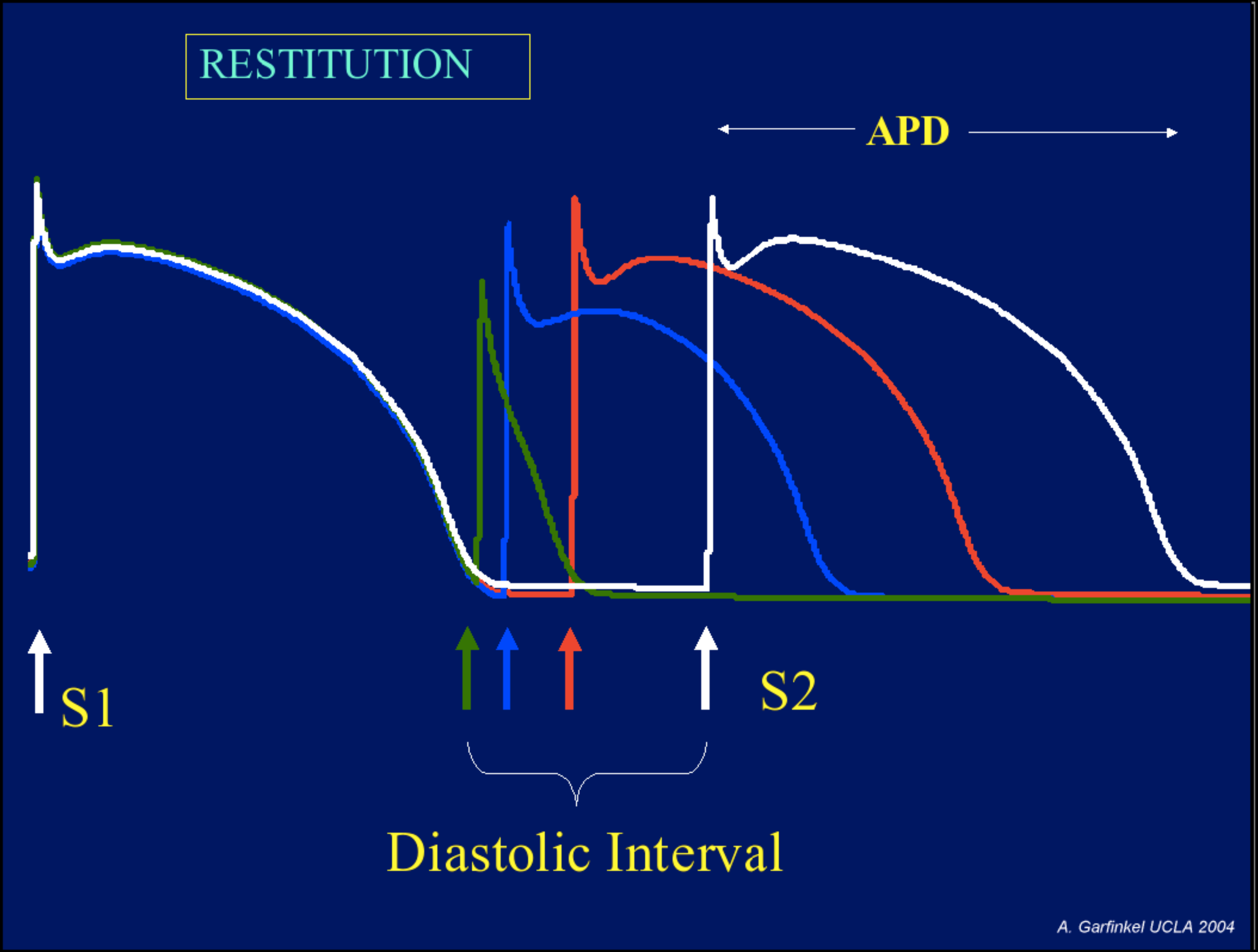
RESTITUTION
APD
S1
S2
Diastolic Interval
A. Garfinkel UCLA 2004

APD Restitution Curve

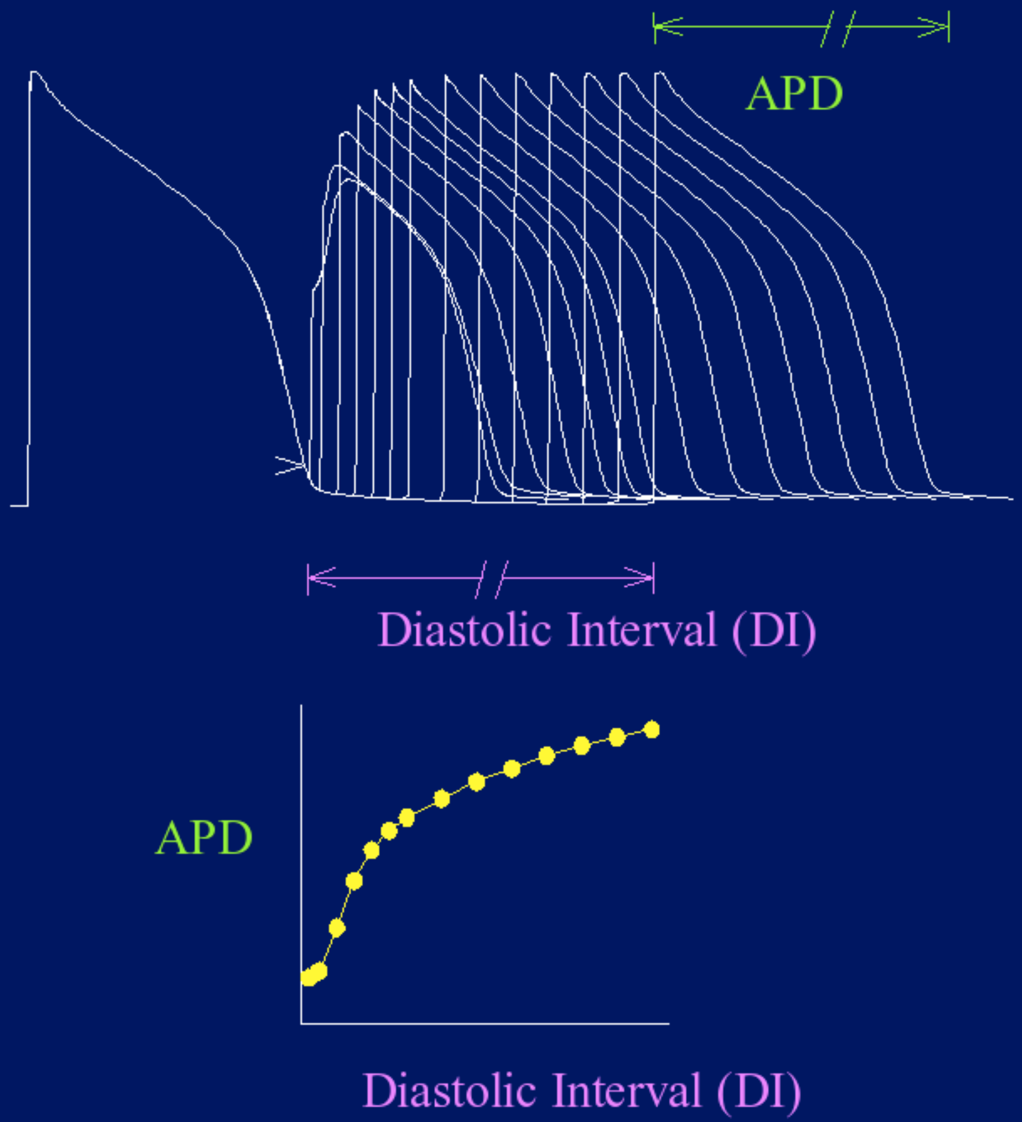

A. Garfinkel UCLA 2004

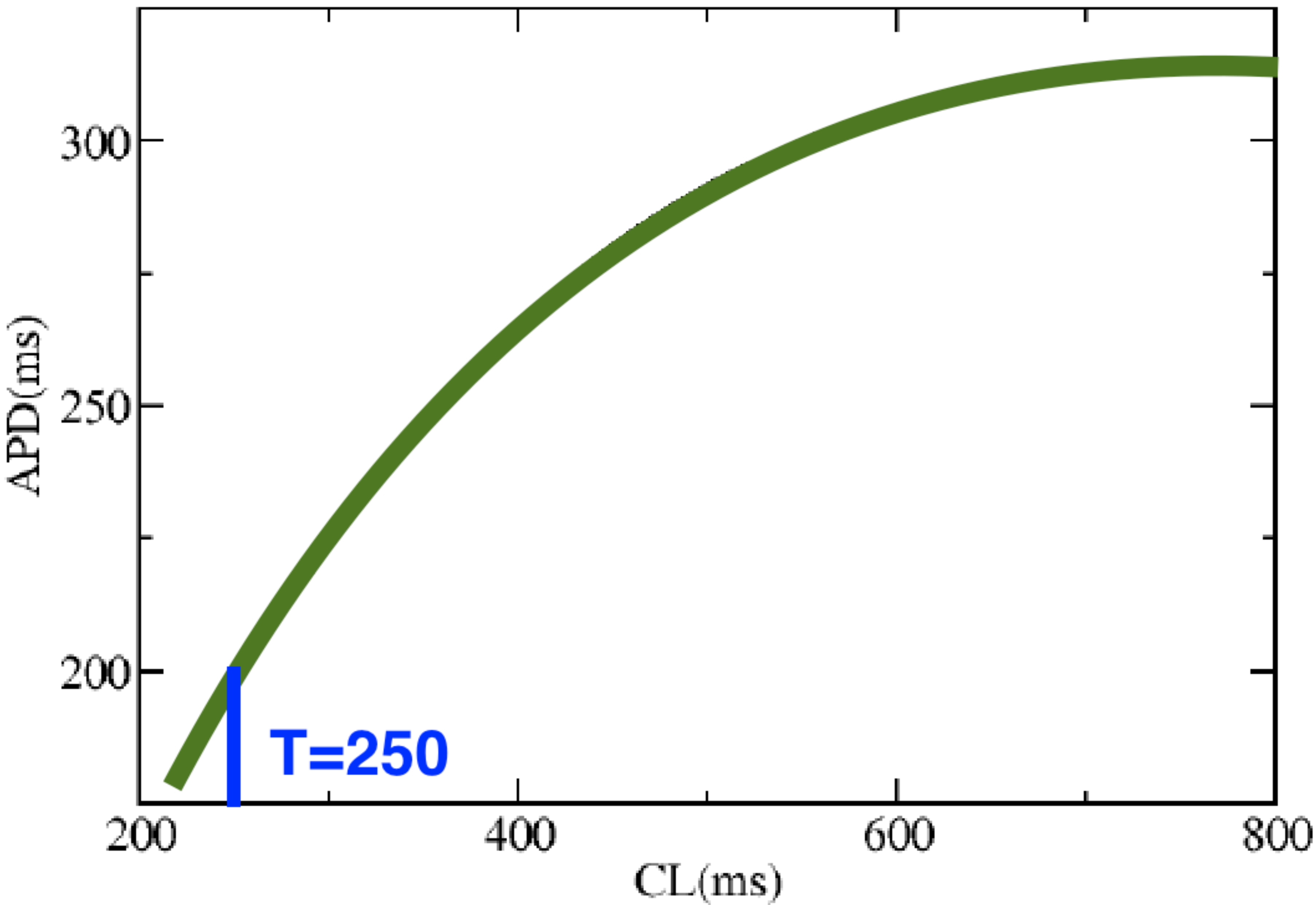

APD(ms)
300
250
200
T=250
200
400
600
800
CL(ms)

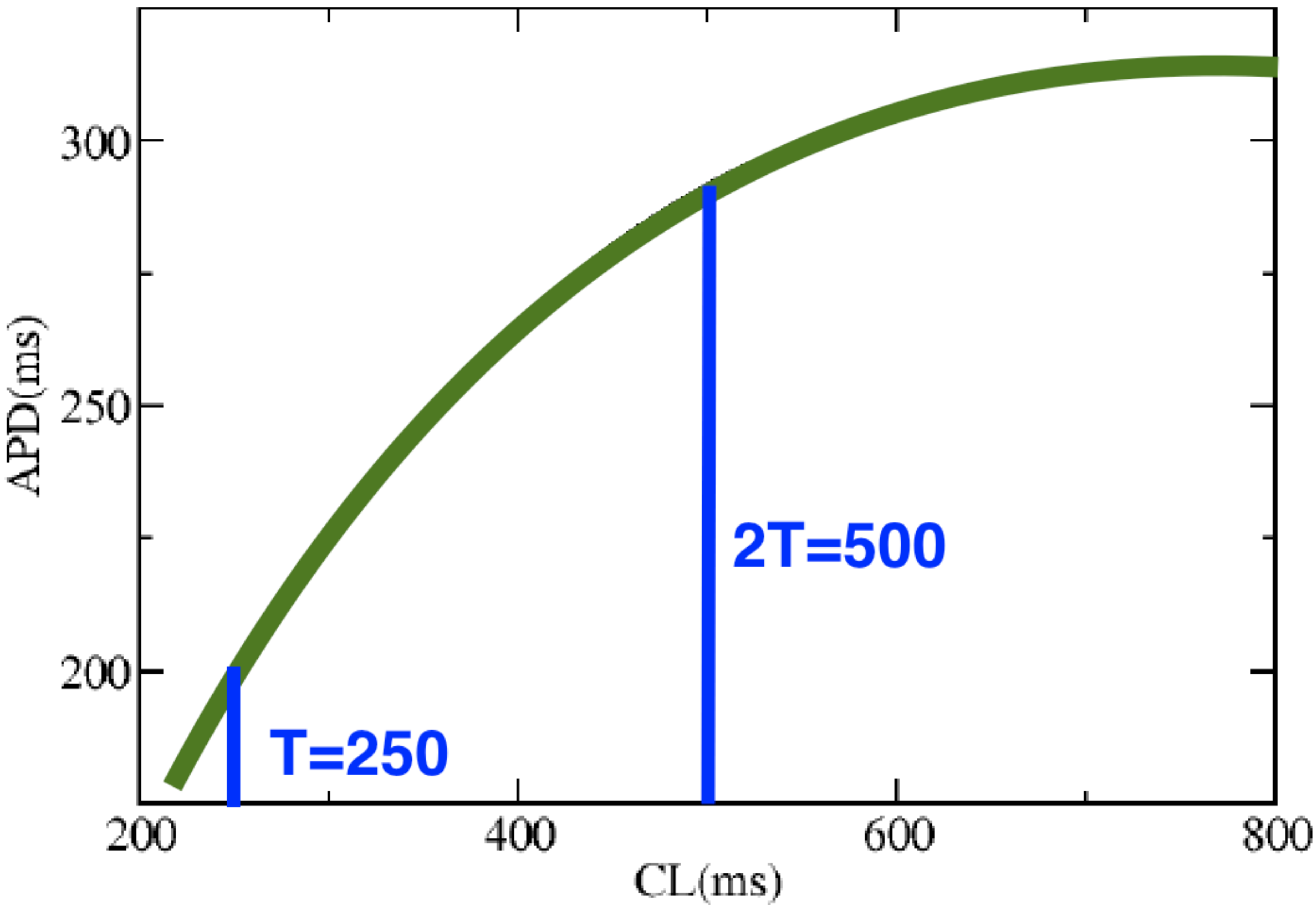

300
250
200
APD(ms)
200
400
600
800
CL(ms)
2T=500
T=250

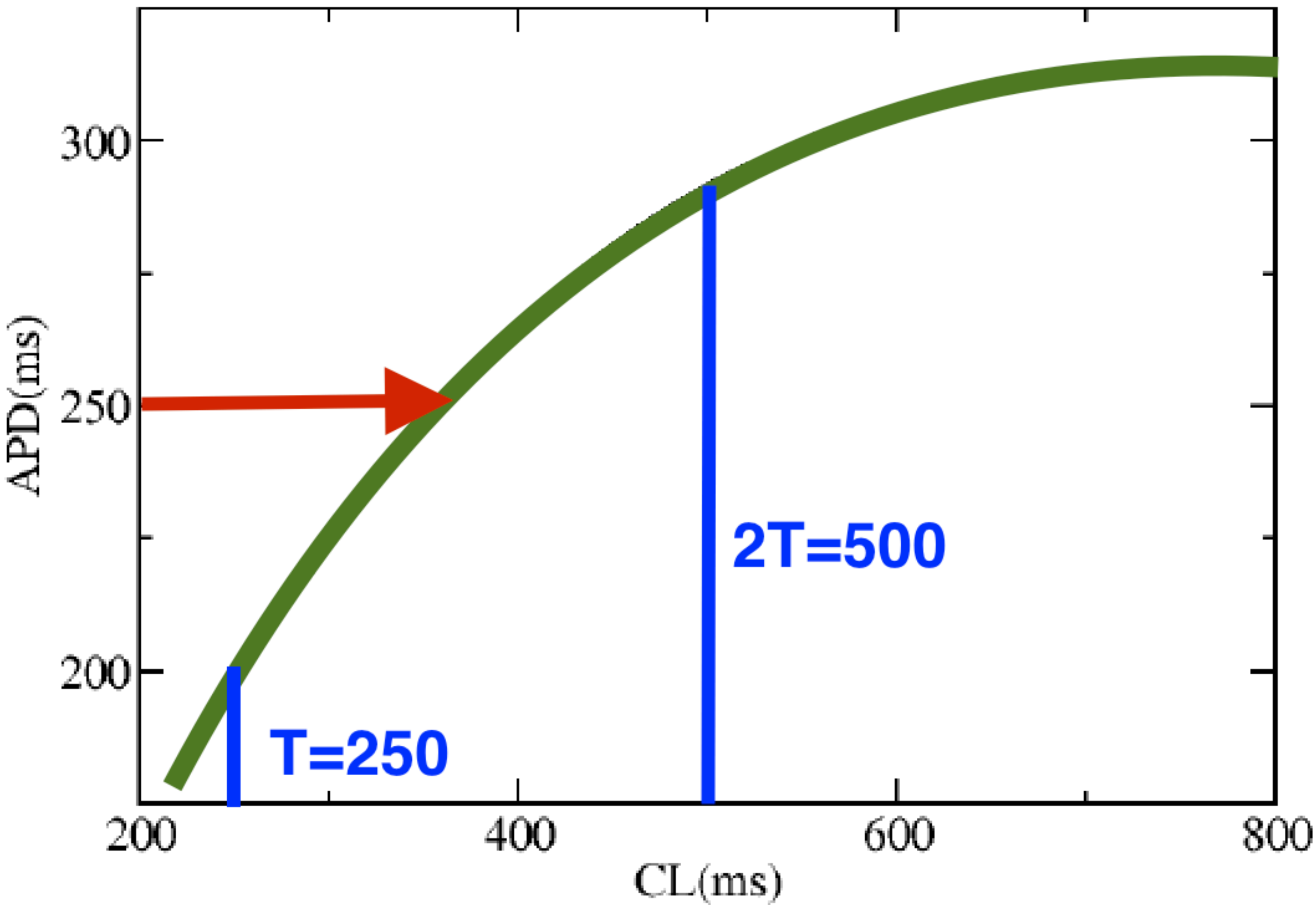
300
250
200
APD(ms)
200
400
600
800
CL(ms)
T=250
2T=500

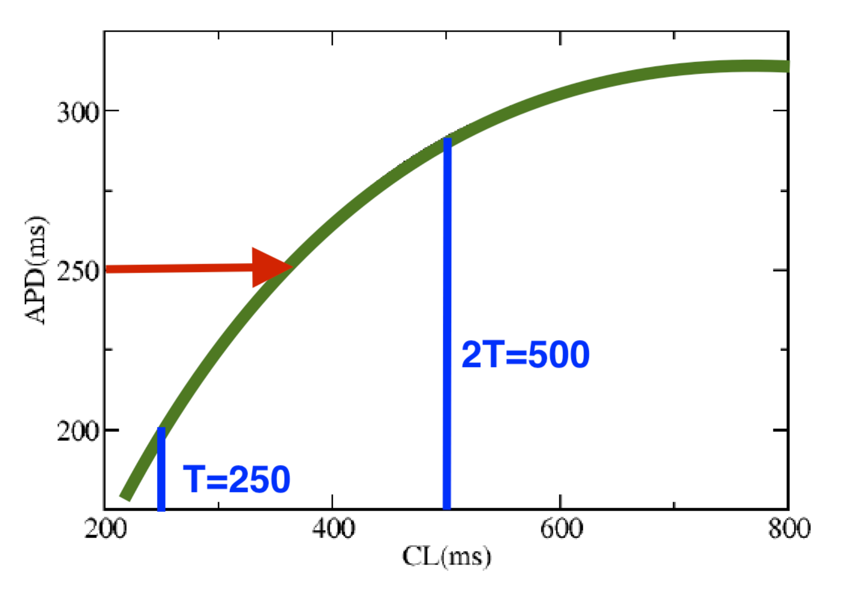
300
250
200
APD(ms)
200
400
600
800
CL(ms)
2T=500
T=250

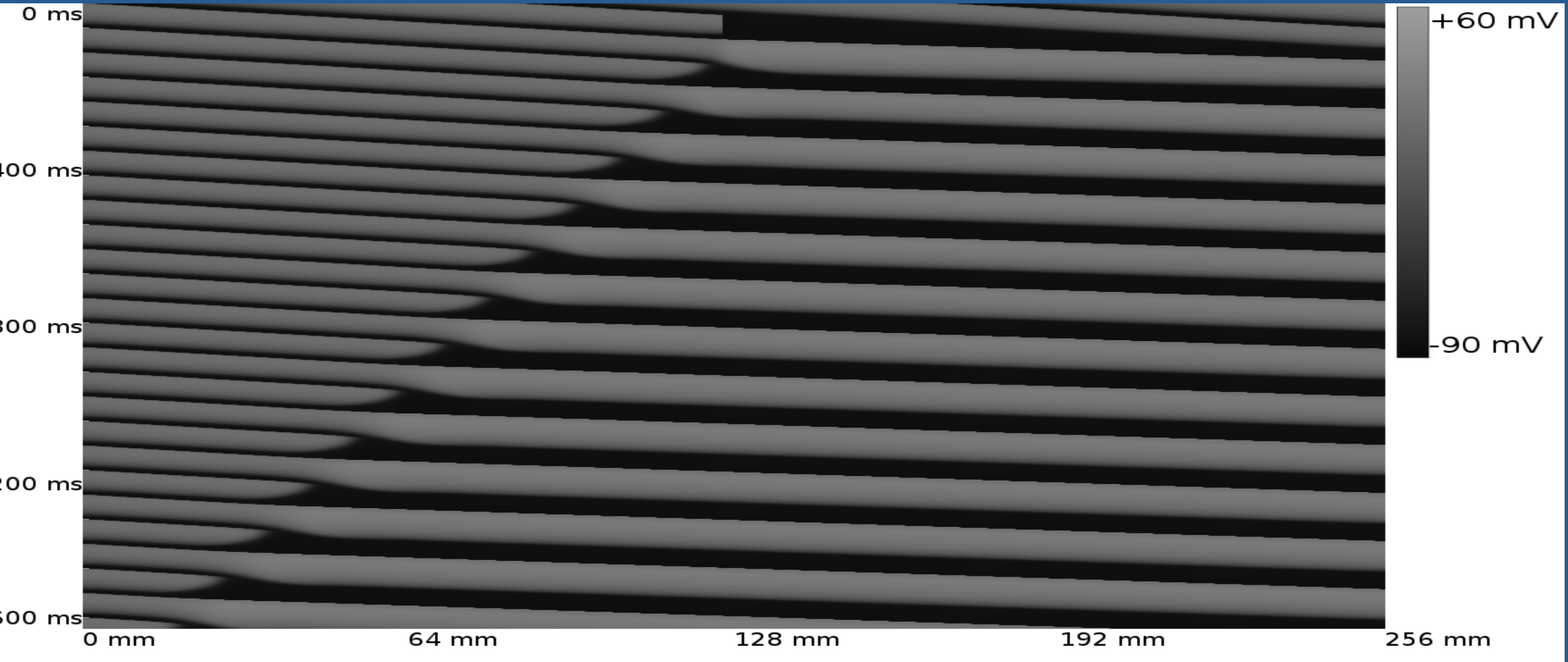
0 ms
400 ms
800 ms
200 ms
600 ms
0 mm
64 mm
128 mm
192 mm
256 mm
+60 mV
-90 mV

$$T'_{n+1}(x_i) = T + \sum_{j=0}^{i} \frac{\Delta x}{CV(DI_{n+1}(x_j))} - \sum_{j=0}^{i} \frac{\Delta x}{CV(DI_{n+1}(x_j))}$$

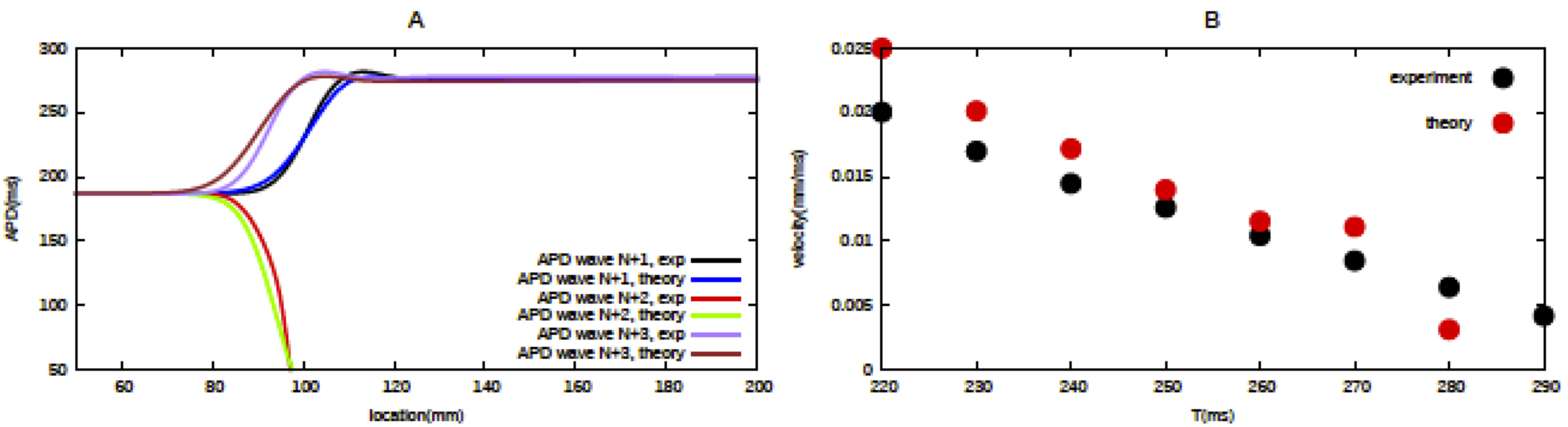

LINK

LINK

[LINK]

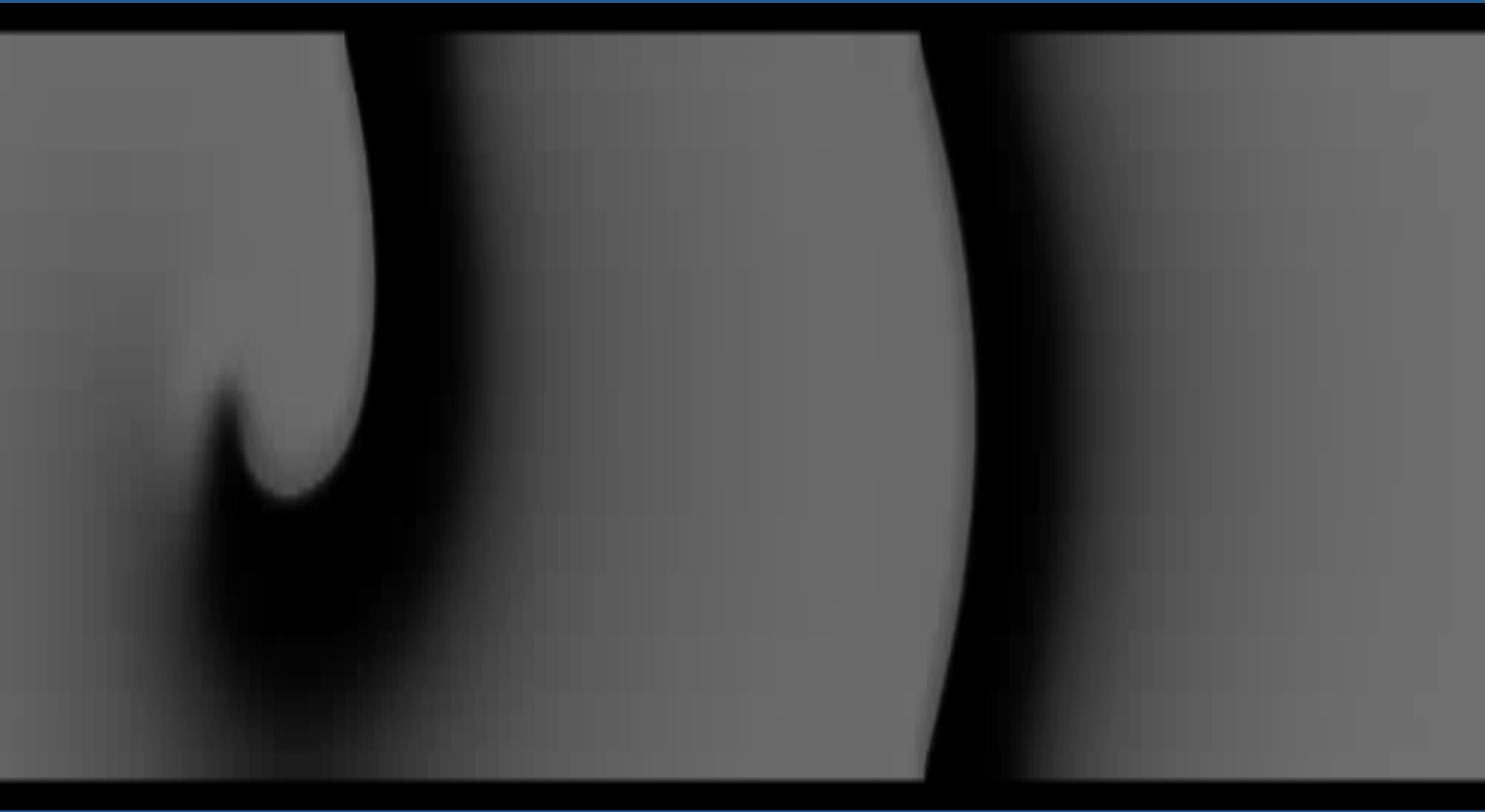

LINK

Conclusions

Small sized heterogeneities attract rotors
via dynamical anchoring

Scars surrounded by the fibrotic regions attract rotors

Dynamical anchoring occurs due to spread of wavelets,
which may be cause by the global alternans instability

Acknowledgments

Numerical simulation were performed by I. Kazbanov, Nele Vandersickel, Kirsten Ten Tusscher, Rupamanjari Majumder

We are thankfull J. de Bakker for for help in the research